

## **Supplementary Figures and Tables**

### **Marker-free coselection for successive rounds of prime editing in human cells**

Sébastien Levesque<sup>1,2</sup>, Diana Mayorga<sup>1,2</sup>, Jean-Philippe Fiset<sup>1,2</sup>, Claudia Goupil<sup>1,2</sup>, Alexis Durringer<sup>1,2</sup>, Andréanne Loiselle<sup>1,2</sup>, Eva Bouchard<sup>1,2</sup>, Daniel Agudelo<sup>1,2</sup>, Yannick Doyon<sup>1,2\*</sup>

<sup>1</sup>Centre Hospitalier Universitaire de Québec Research Center - Université Laval, Québec, QC, G1V 4G2, Canada.

<sup>2</sup>Université Laval Cancer Research Centre, Québec, QC, G1V 0A6, Canada.

\*Correspondence:

Yannick Doyon, Ph.D.

Centre de recherche du CHU de Québec – Université Laval

2705, boulevard Laurier, T-3-67

Québec, QC G1V 4G2

CANADA

Tel: 418-525-4444 ext. 46264

e-mail: [Yannick.Doyon@crchudequebec.ulaval.ca](mailto:Yannick.Doyon@crchudequebec.ulaval.ca)

ORCID 0000-0002-3889-9563

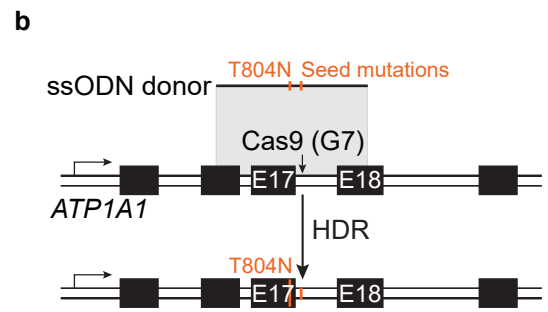
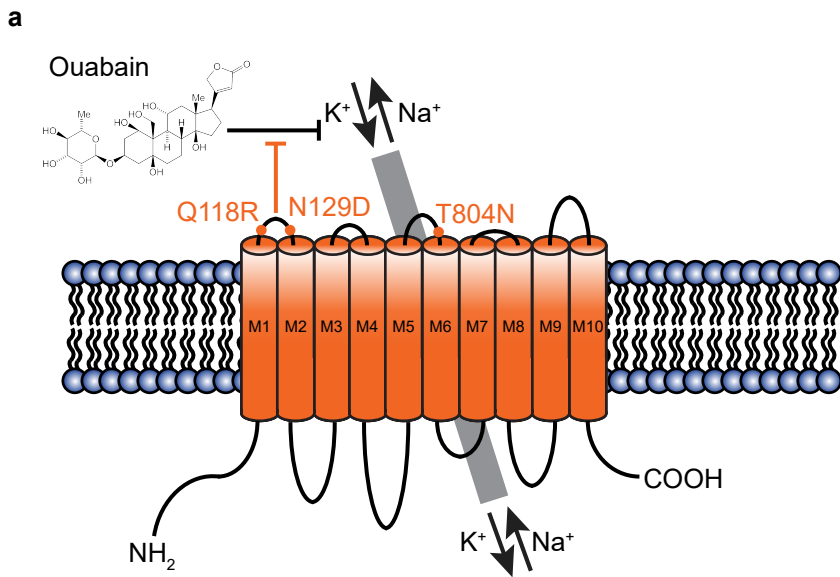
### **Supplementary figures**

1. Targeting *ATPIA1* exon 17 induces cellular resistance to ouabain
2. *ATPIA1* as a selectable genomic harbor for targeted integration of transgenes
3. Targeting *ATPIA1* repeatedly for successive gene knock-in and gene tagging
4. Targeting *ATPIA1* repeatedly allows up to three sequential steps of selection
5. Coselection for adenine base editing
6. Prime editing at the *ATPIA1* locus confers resistance to ouabain
7. Prime editing at *ATPIA1* does not impact cell fitness nor *ATPIA1* steady-state levels
8. Robust coselection for prime editing in HeLa S3 cells
9. Detection of PE3-mediated translocations in K562 cells
10. Coselection for HDR or PE using an EBFP to EGFP reporter system
11. *ATPIA1* as a selectable genomic harbor for targeted integration of a mTORC1 signaling reporter
12. mSc-TOSI reporter intensity in bulk coselected populations of K562 cells
13. PE3-induced indels at *MTOR* and *ATPIA1* in single cell-derived clones
14. Large PE3-mediated insertions in single cell-derived clones

15. mSc-TOSI reporter intensity in single cell-derived clones harboring *MTOR* mutations
16. Successive rounds of coselection for the isolation of double *MTOR* mutants
17. Sequential mSc-TOSI knock-in and coselection for prime editing at *MTOR* in HeLa S3 cells
18. Engineered pegRNAs (epegRNAs) with MMR-evading mutations enhance prime editing at *ATP1A1*
19. Robust coselection for prime editing at *MTOR* in U2OS cells with engineered pegRNAs
20. Characterization of large PE3-mediated insertions in bulk populations of HeLa S3 cells
21. Assessing the impact of 53BP1 inhibition on large PE-mediated insertions
22. Assessing the impact of complementary-strand nick locations on prime editing outcomes
23. Representative FACS plots for EBFP to EGFP conversion
24. Assessing the impact of complementary-strand nick locations on prime editing byproducts
25. Gating strategies used during this study.
26. Uncropped scans of all gels and blots from this study.

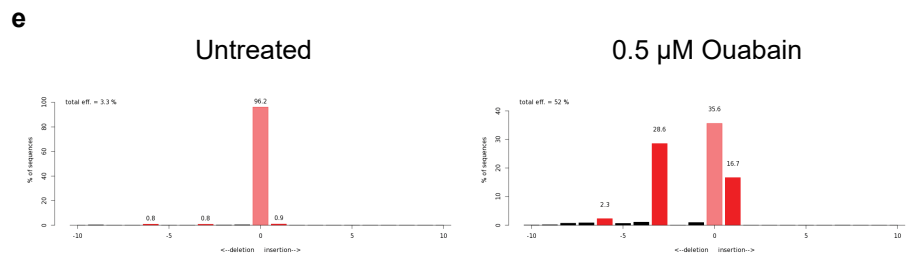
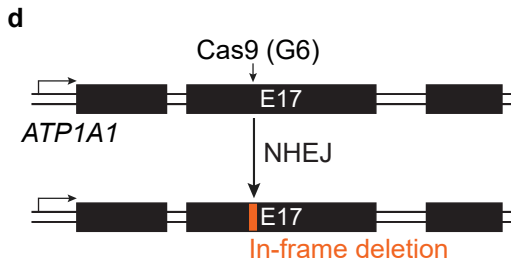
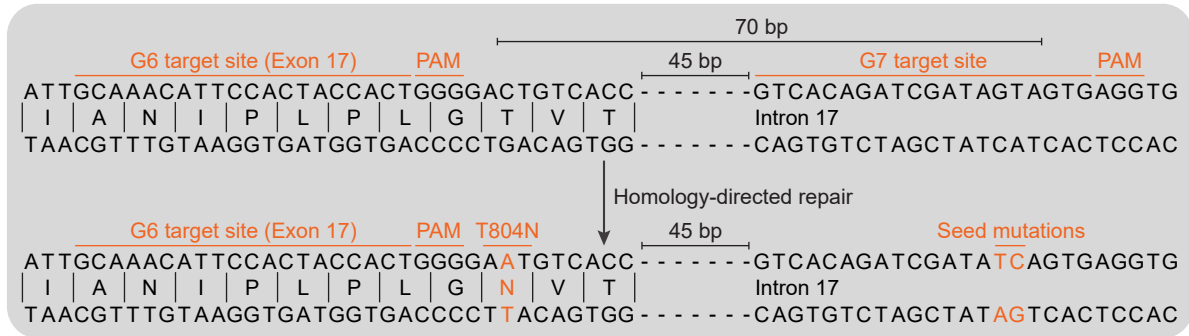
### **Supplementary tables**

1. Distribution of alleles in single cell-derived clones edited at *ATP1A1* via prime editing
2. Distribution of alleles in single cell-derived clones edited at *ATP1A1* and *MTOR* by coselection using engineered pegRNAs (epegRNAs) in PE2 mode.

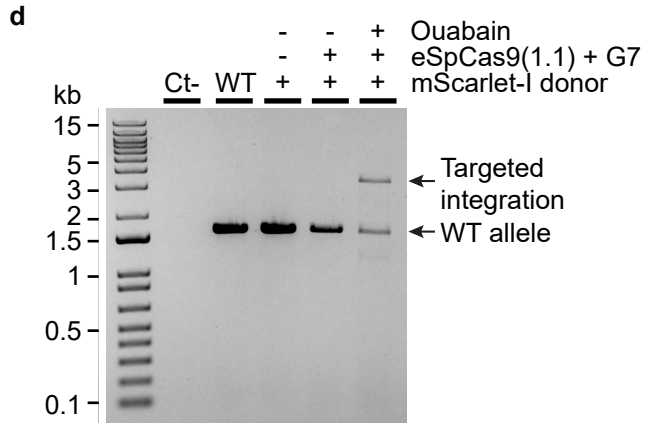
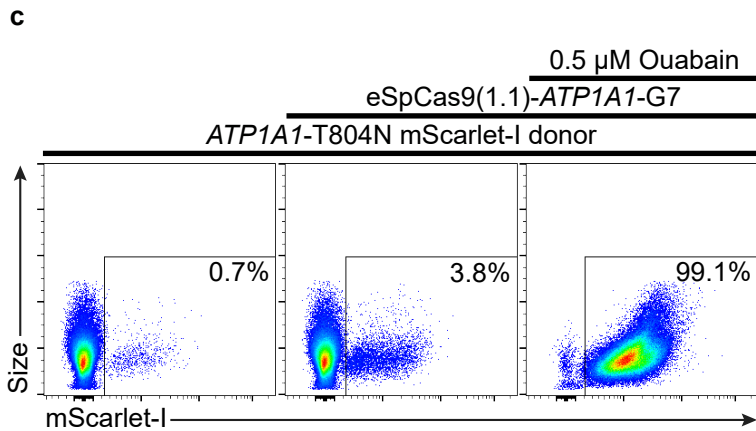
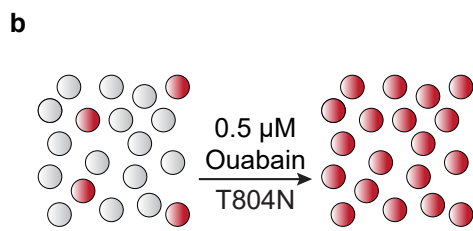
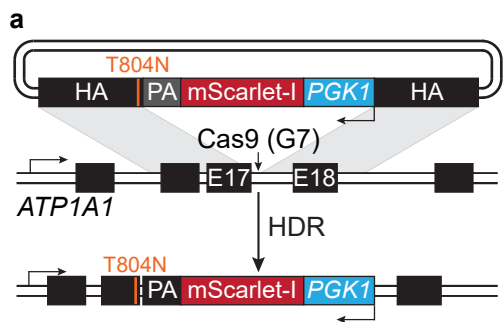


**c**

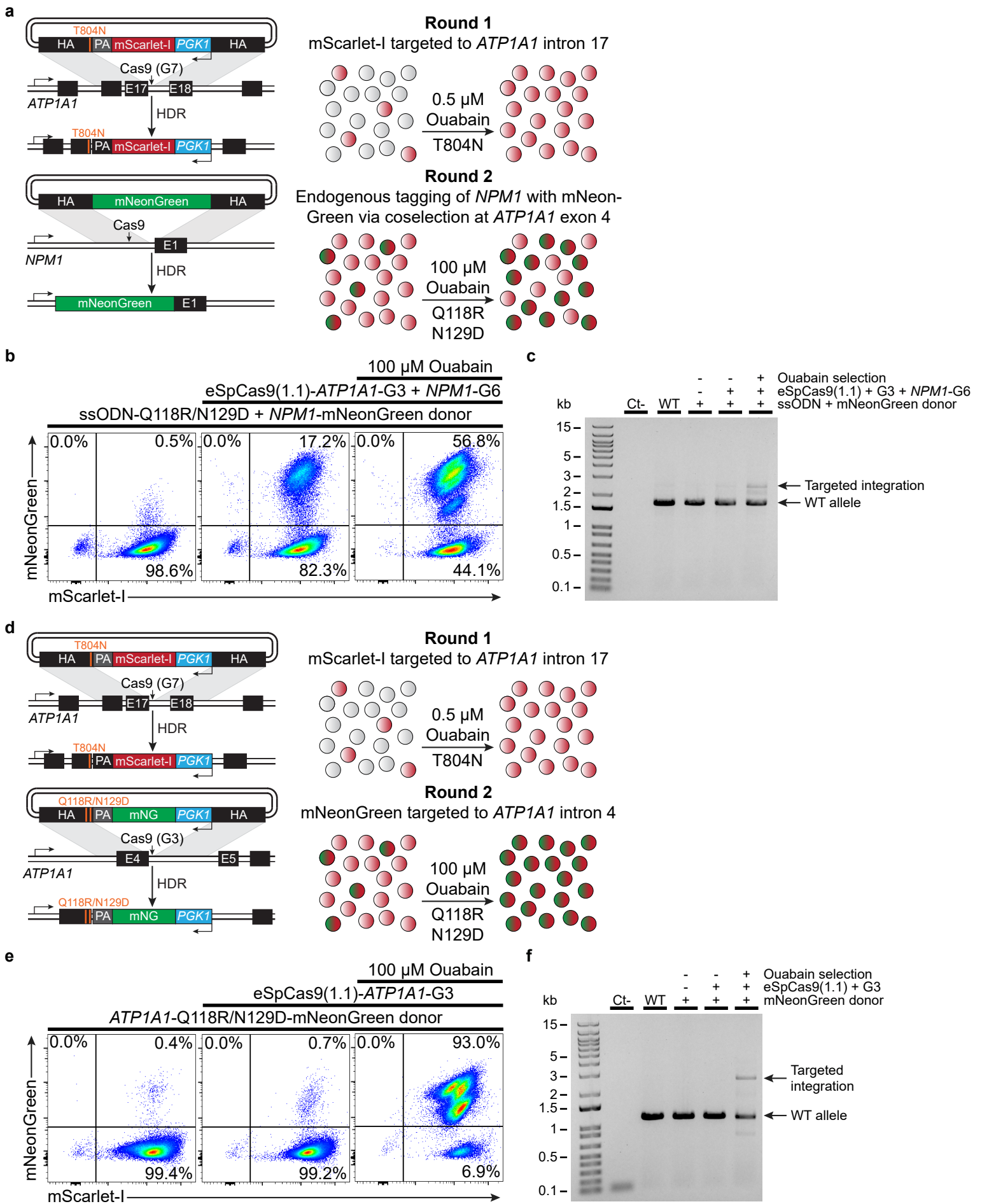
ATP1A1 Exon-Intron 17



**Supplementary figure 1 (Related to Fig. 1). Targeting *ATP1A1* exon 17 induces cellular resistance to ouabain.** (a) Schematic representation of the Na<sup>+</sup>/K<sup>+</sup> ATPase. The first and third extracellular loops are encoded by *ATP1A1* exon 4 and 17, respectively. (b) Schematic of HDR-driven editing at *ATP1A1* exon 17 using a ssODN donor. A DNA double-stranded break is introduced via SpCas9 at *ATP1A1* intron 17 and the T804N mutation is introduced via HDR at exon 17 using a ssODN donor. (c) Schematic representation of SpCas9 target sites used for NHEJ-driven (G6) or HDR-driven (G7) editing at *ATP1A1* exon 17 to induce cellular resistance to ouabain. The exon-intron boundary, and the distance between G7 and the T804 codon are shown. (d) Schematic representation of NHEJ-driven editing *ATP1A1* exon 17. (e) Small indels profile at *ATP1A1* exon 17 following G6-mediated cleavage and ouabain (0.5 μM) selection as determined by TIDE from Sanger sequencing. K562 cells were transfected with an eSpCas9(1.1) vector and treated with or without 0.5 μM ouabain starting 3 days post-transfection until all non-resistant cells were eliminated. *n* = 1 experiment.

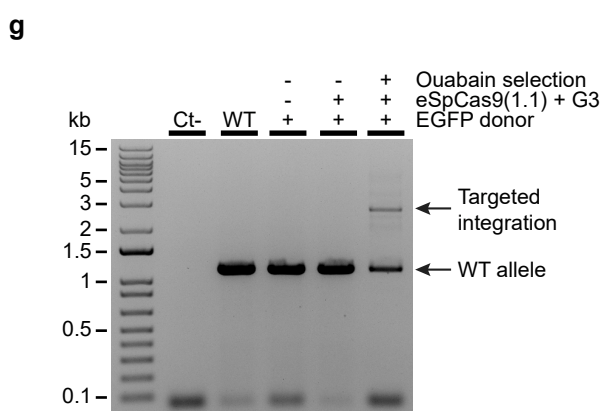
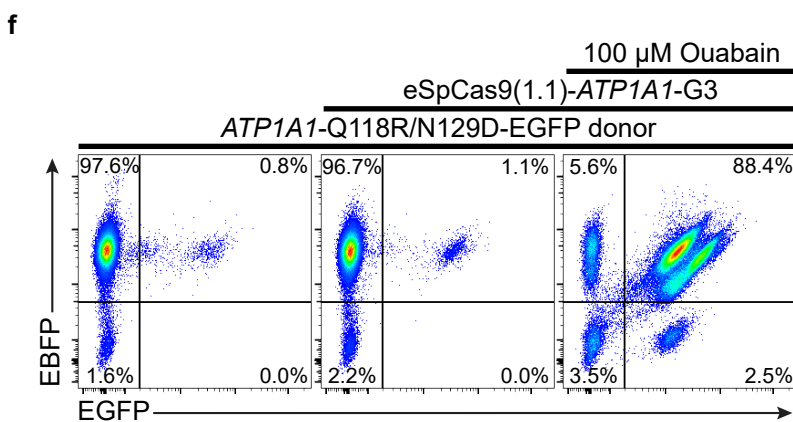
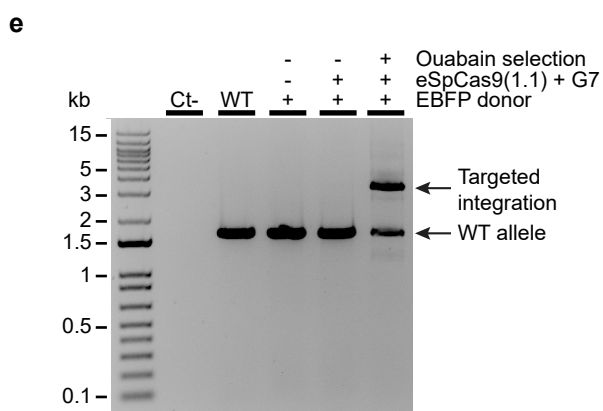
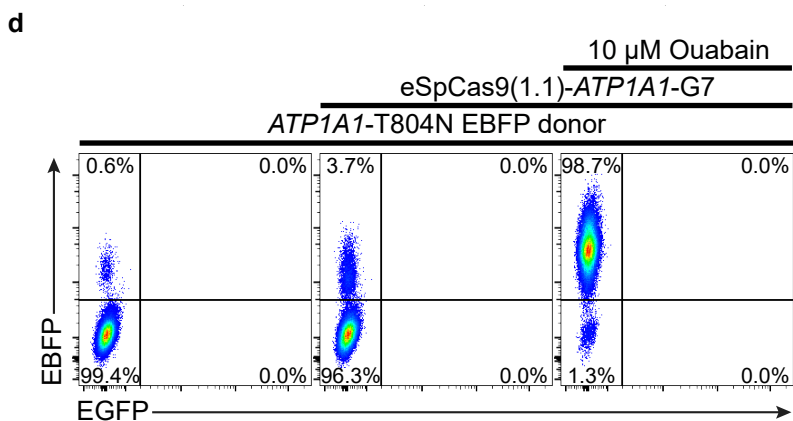
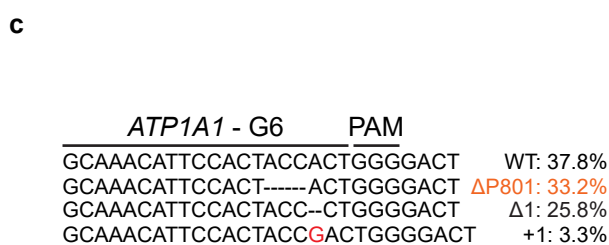
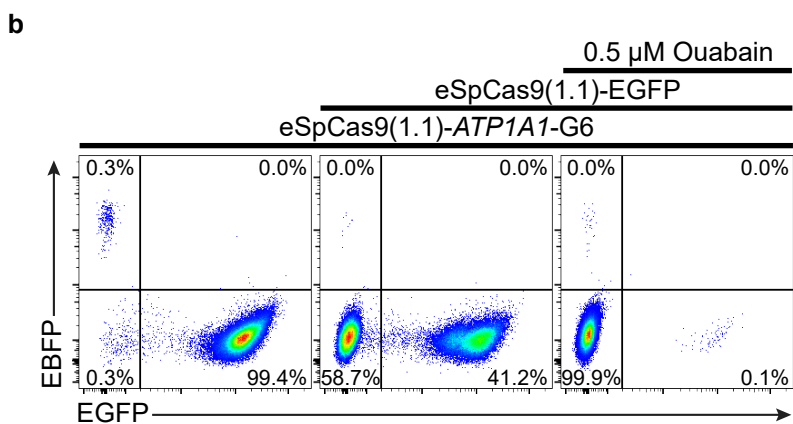
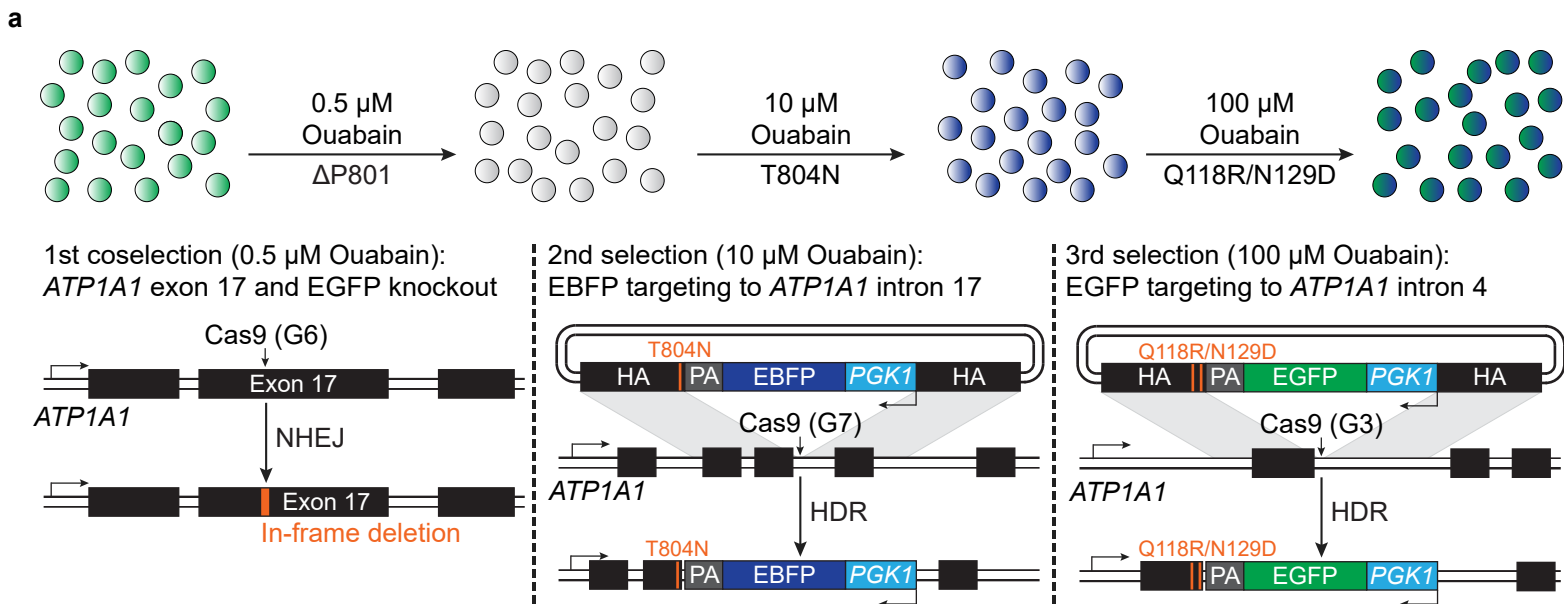


**Supplementary figure 2. *ATP1A1* as a selectable genomic harbor for targeted integration of transgenes.** (a) Schematic representation of mScarlet-I targeting to the reverse DNA strand of the *ATP1A1* locus. The T804N mutation is introduced via the left homology arm (HA) and transgene expression is driven by a human *PGK1* promoter. (b) Schematic of direct selection for targeted integration at *ATP1A1*. (c) FACS-based quantification of mScarlet-I knock-in at *ATP1A1* intron 17. K562 cells were transfected with eSpCas9(1.1) and a donor targeting *ATP1A1* and treated with or without 0.5  $\mu$ M ouabain 3 days post-transfection until all non-resistant cells were eliminated. (d) Out-Out PCR for mScarlet-I knock-in detection at *ATP1A1* intron 17.  $n = 1$  experiment.



**Supplementary figure 3. Targeting *ATPIA1* repeatedly for successive gene knock-in and gene tagging.** (a) Schematic representation of mScarlet-I targeting to the reverse DNA strand of the *ATPIA1* locus. The T804N mutation is introduced via the left homology arm (HA) and transgene expression is driven by a human *PGKI* promoter. Following the first selection step with a mutation that confers a medium level of resistance to ouabain (T804N), a sequential step of coselection for *NPM1* tagging with mNeonGreen is performed with a higher concentration of ouabain. (b) FACS-based quantification of targeted mScarlet-I integration at *ATPIA1* intron 17 and *NPM1* tagging with mNeonGreen. K562 cells stably expressing mScarlet-I (see **Supplementary Fig. 2**) were transfected with nuclease vectors and donors targeting *ATPIA1* and *NPM1* and treated with or without 100  $\mu$ M ouabain 3 days post-transfection until all non-resistant cells were eliminated. (c) Out-Out PCR for mNeonGreen knock-in detection at *NPM1*.  $n = 1$  experiment. (d) Same as in (a), but sequential gene knock-in at the *ATPIA1* locus. Following mScarlet-I knock-in at *ATPIA1* intron 17, a sequential mNeonGreen knock-in to *ATPIA1* exon 4 is performed with 100  $\mu$ M ouabain. (e) FACS-based quantification of successive targeted integrations of mScarlet-I and mNeonGreen at *ATPIA1* intron 17 and 4, respectively. K562 cells stably expressing mScarlet-I (see **Supplementary Fig. 2**) were transfected with eSpCas9(1.1) and a donor targeting *ATPIA1* and treated with 100  $\mu$ M ouabain 3 days post-transfection until all non-resistant cells were eliminated. (f) Out-Out PCR for mNeonGreen knock-in detection at *ATPIA1* intron 4.  $n = 1$  experiment. *PGKI*, human phosphoglycerate kinase 1 promoter. PA, polyadenylation signal. HA, homology arm. E4 and E17, exon 4 and exon 17. mNG, mNeonGreen.

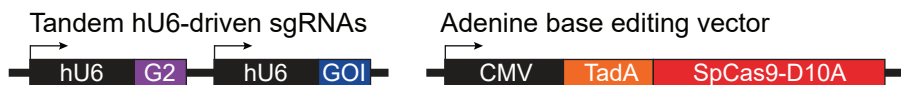
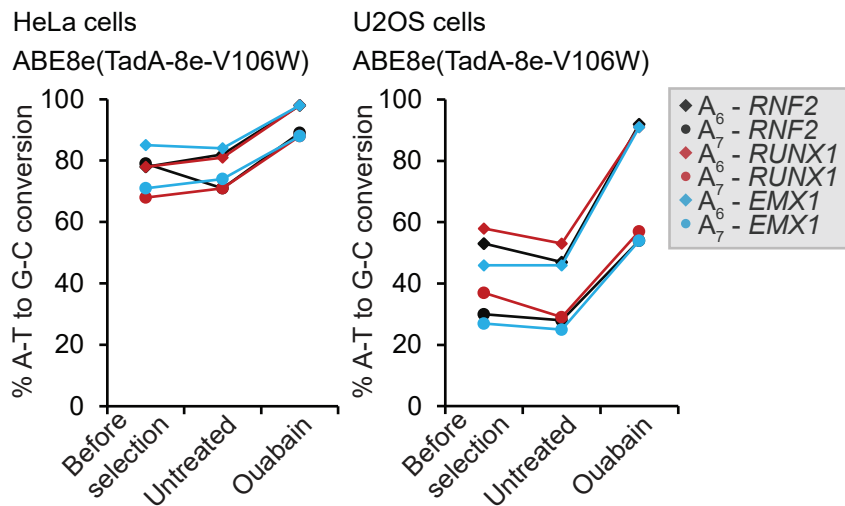
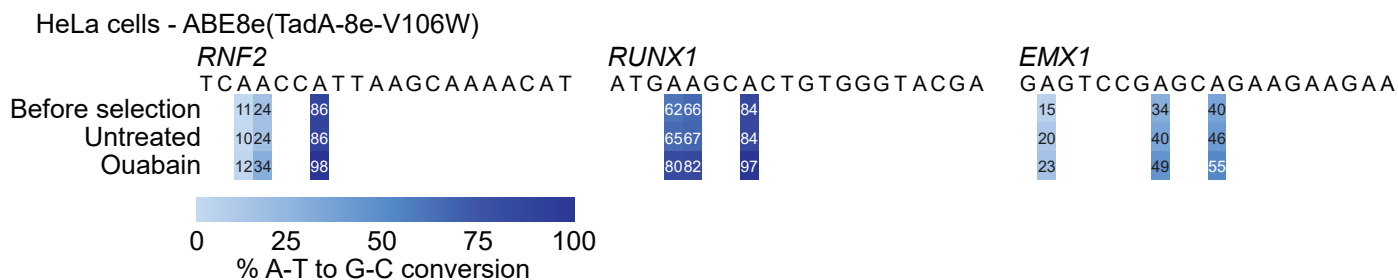
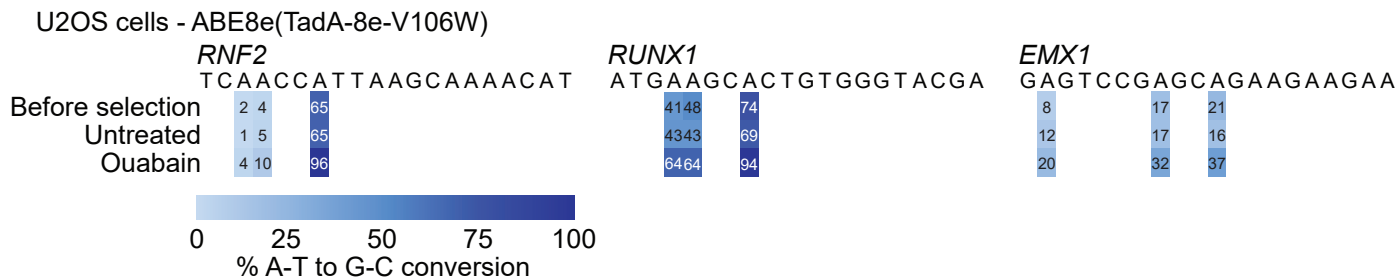




**Supplementary figure 4. Targeting *ATP1A1* repeatedly allows up to three sequential steps of selection.** (a) Schematic representation of the three steps of marker-free selection. An in-frame deletion is first introduced to *ATP1A1* exon 17 via NHEJ allowing the coselection for NHEJ events at a distant locus of interest represented by EGFP. Then, sequential targeting of expression cassettes for fluorescent proteins to *ATP1A1* introns 17 and 4 is performed by increasing the dose of ouabain at each step. (b) FACS-based quantification for EGFP knockout. K562 cells stably expressing EGFP from the *AAVS1* locus were transfected with nuclease vectors targeting *ATP1A1* and EGFP and treated with or without 0.5  $\mu$ M ouabain 3 days post-transfection until all non-resistant cells were eliminated. (c) DECODR Sanger sequencing trace analysis of *ATP1A1* exon 17 following coselection for EGFP knockout.  $n = 1$  experiment. (d) FACS-based quantification for EBFP knock-in at *ATP1A1* intron 17. Following the first step of selection, coselected K562-EGFP knockout cells were transfected with eSpCas9(1.1) and a donor to target an EBFP expression cassette to *ATP1A1* intron 17 and treated with 10  $\mu$ M ouabain 3 days post-transfection until all non-resistant cells were eliminated. (e) Out-Out PCR for EBFP knock-in detection at *ATP1A1* intron 17.  $n = 1$  experiment. (f) FACS-based quantification for EGFP knock-in at *ATP1A1* intron 4. Following EGFP knockout and EBFP knock-in, K562 cells were transfected with eSpCas9(1.1) and a donor to target an EGFP expression cassette to *ATP1A1* intron 4 and treated with or without 100  $\mu$ M ouabain 3 days post-transfection until all non-resistant cells were eliminated. (g) Out-Out PCR for EGFP knock-in detection at *ATP1A1* intron 4.  $n = 1$  experiment. *PGK1*, human phosphoglycerate kinase 1 promoter. PA, polyadenylation signal. HA, homology arm. E4 and E17, exon 4 and exon 17.

**a**

*ATP1A1-G2*  
 GATCCA<sub>6</sub>A<sub>7</sub>GCTGCTACAGAAG  
 CAA to CAG: Silent mutation  
 CAA to CGA: Q118R  
 CAA to CGG: Q118R

**b****c****d****e**

**Supplementary figure 5. Coselection for adenine base editing.** (a) Putative adenine base editing outcomes at *ATP1A1* exon 4 with SpCas9 *ATP1A1*-G2 (b) Schematic representation of the dual-sgRNA vector targeting *ATP1A1* and a gene of interest (GOI), and the adenine base editing vector. (c) Adenine base editing quantification at *ATP1A1* exon 4 (Q118R) from three experiments co-targeting *RNF2*, *RUNX1*, and *EMX1*, as determined by BEAT analysis from Sanger sequences. HeLa S3 or U2OS cells were transfected with adenine base editing and sgRNA-expressing vectors and treated with or without 0.5  $\mu$ M ouabain for 10 days starting 3 days post-transfection. (d) Same as in (c) for adenine base editing at coselected GOIs in HeLa S3 cells. (e) Same as in (d) with U2OS cells.  $n = 1$  experiment.

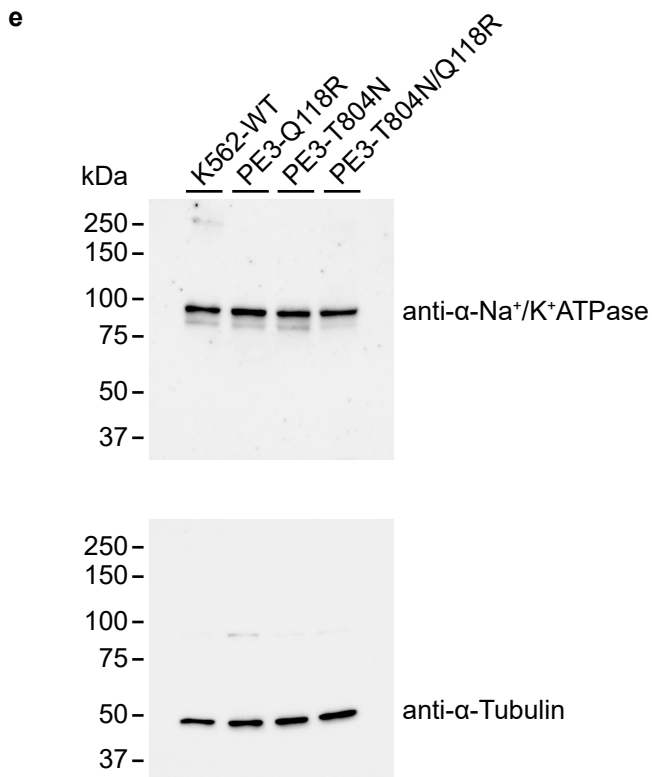
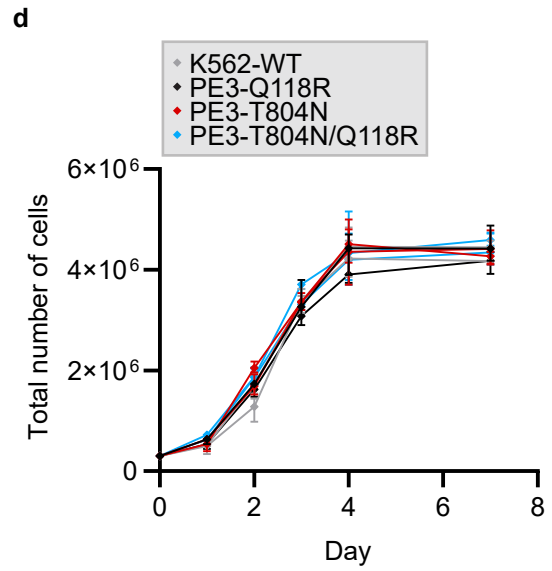
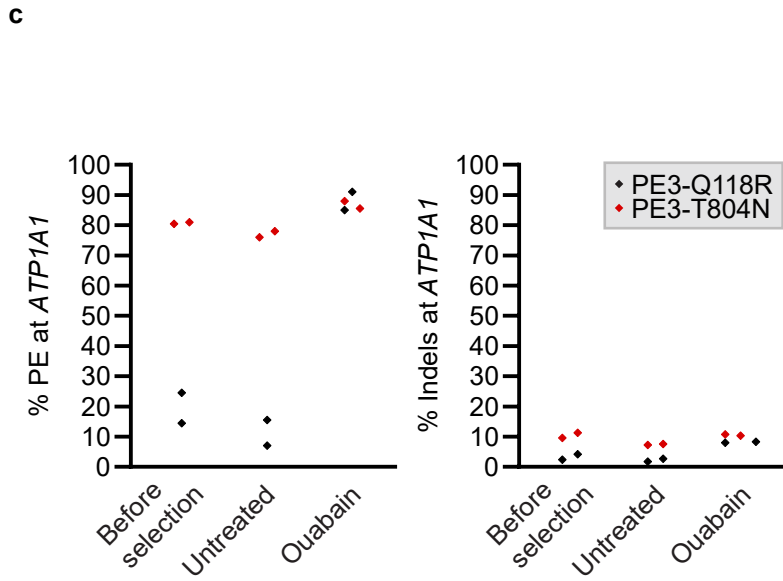
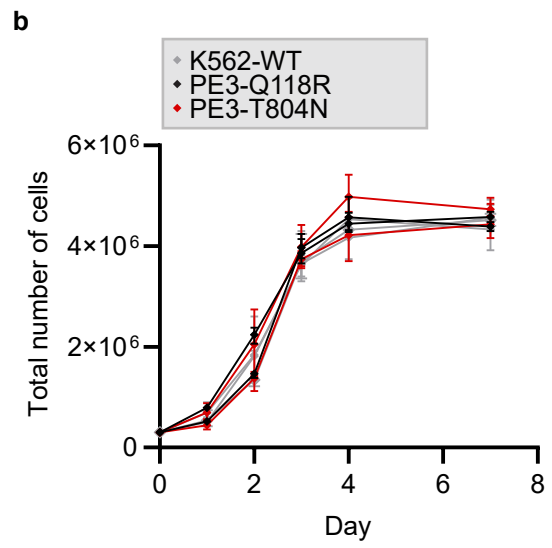
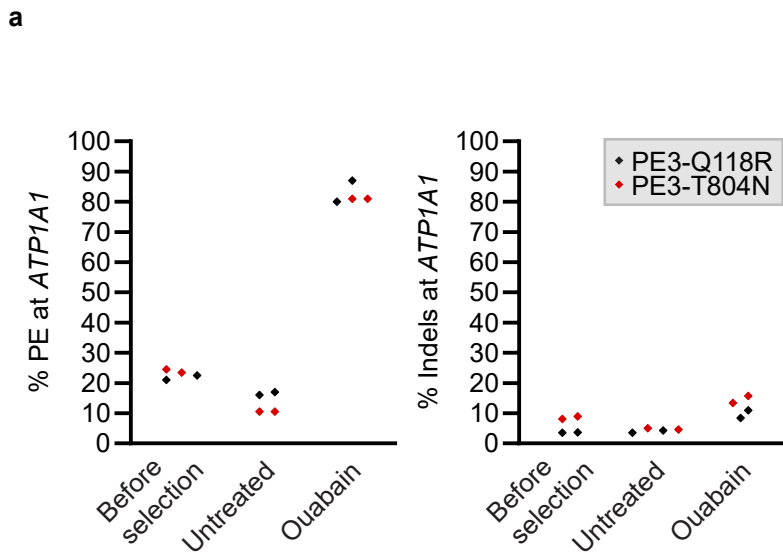


**Supplementary figure 6. Prime editing at the *ATP1A1* locus confers resistance to ouabain.**

**(a)** Schematic representation of the SpCas9 target sites and the reverse transcriptase (RT) template used to install the T804N mutation at *ATP1A1* exon 17 to induce cellular resistance to ouabain.

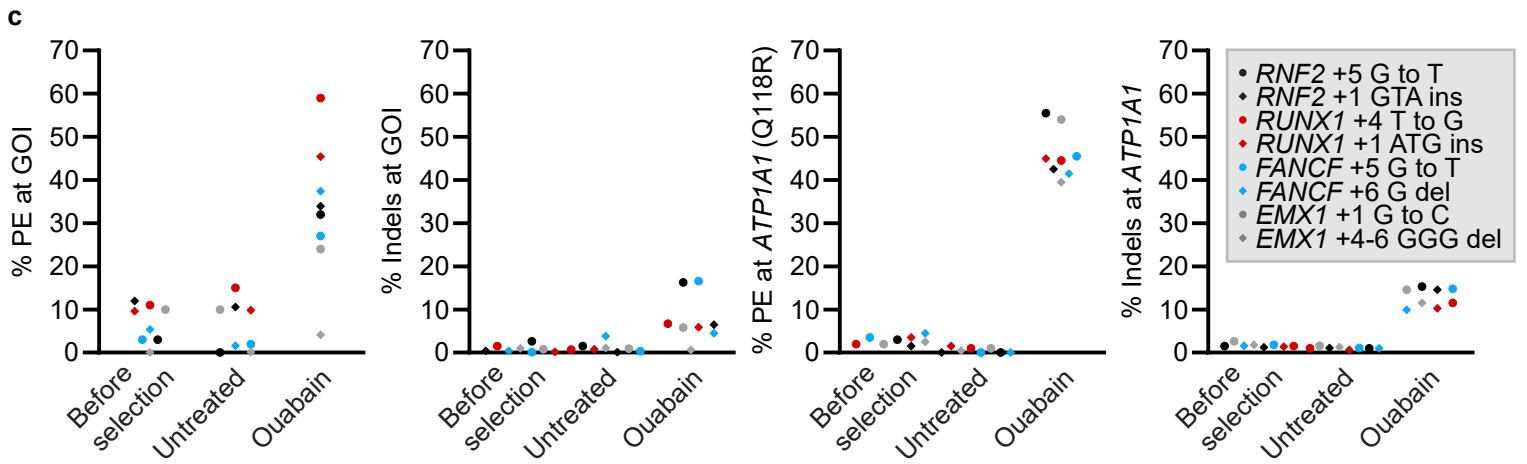
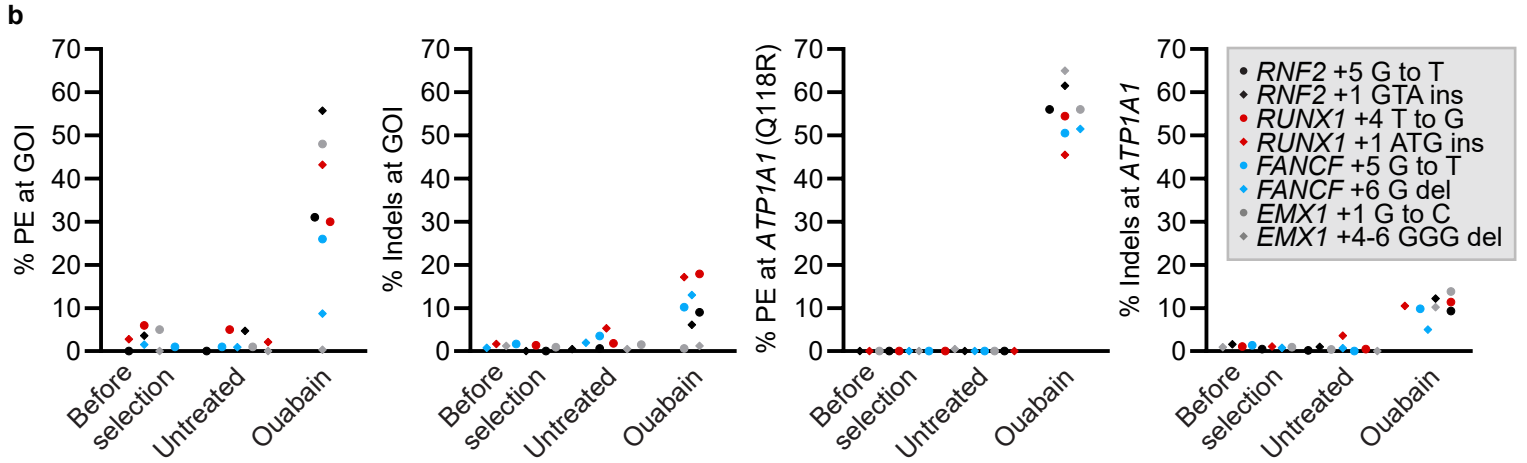
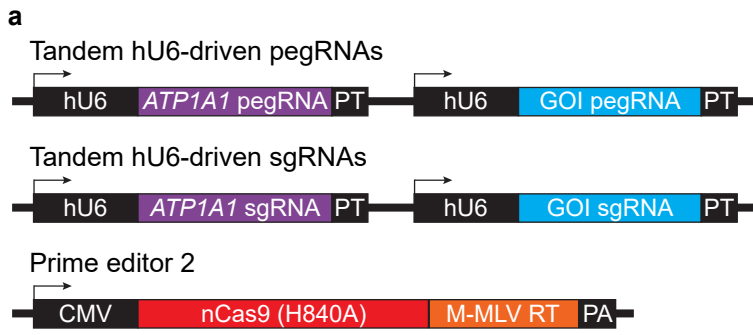
**(b)** Schematic representation of the SpCas9 target sites and the reverse transcriptase (RT) template used to install the Q118R mutation at *ATP1A1* exon 4 to induce cellular resistance to ouabain.

**(c)** PE and small indels quantification at *ATP1A1* as determined by BEAT and TIDE analysis from Sanger sequences. K562 cells were transfected with PE3 vectors and genomic DNA was harvested 3 days post-transfection (before selection) and cells were treated (ouabain) or not (untreated) with 0.5  $\mu$ M ouabain for 10 days starting 3 days post-transfection.  $n = 3$  independent biological replicates performed at different times.

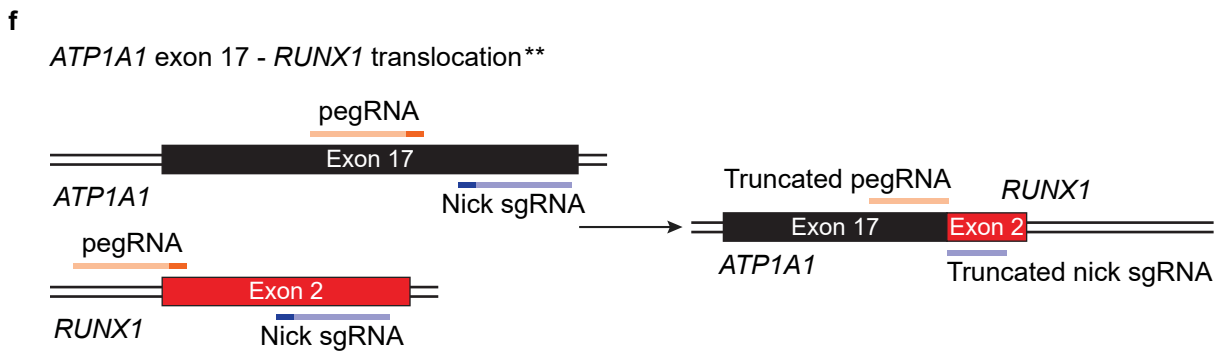
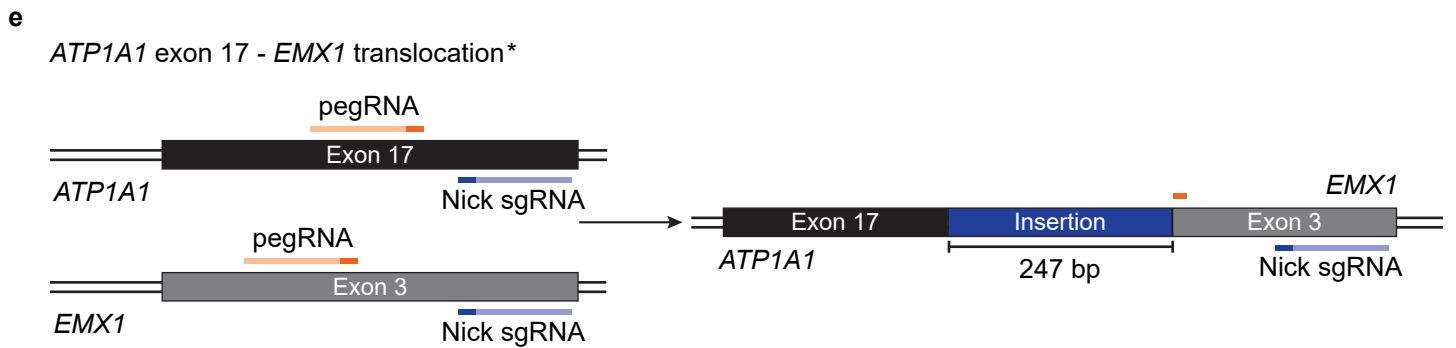
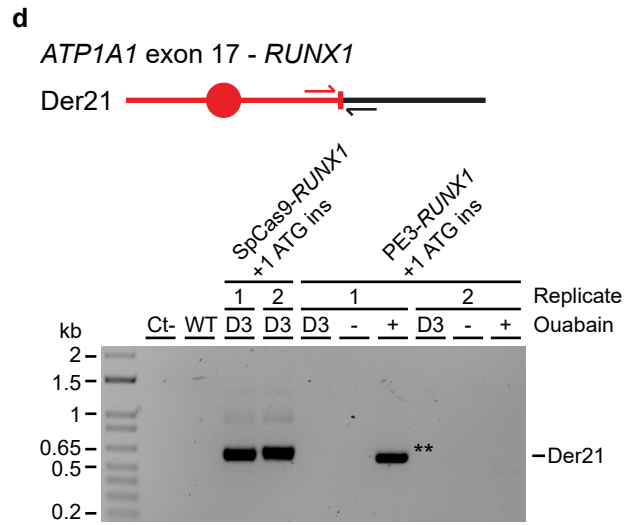
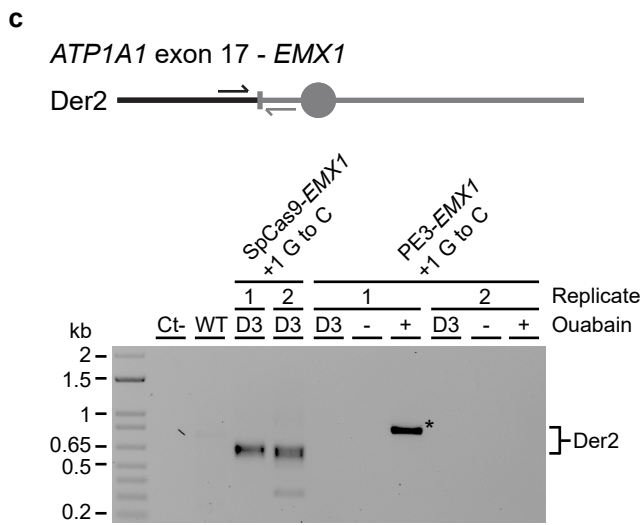
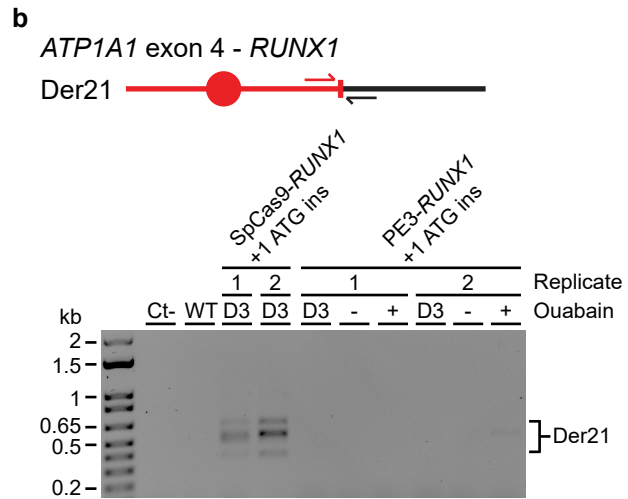
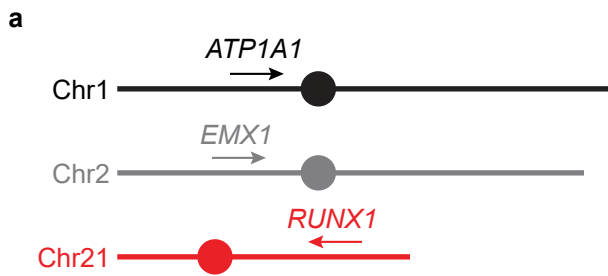


**Supplementary figure 7. Prime editing at *ATP1A1* does not impact cell fitness nor *ATP1A1* steady-state levels.** (a) PE and small indels quantification as determined by BEAT and TIDE analysis from Sanger sequencing. K562 cells were transfected with PE3 vectors targeting *ATP1A1*. Genomic DNA was harvested 3 days post-transfection (before selection) and cells were treated (ouabain) or not (untreated) with 0.5  $\mu$ M ouabain until all non-resistant cells were eliminated. (b) Cell proliferation curves of K562 wildtype (WT) and bulk populations of ouabain-resistant (PE3-Q118R and PE3-T804N) cells. Following ouabain selection, cells were seeded at 75 000 cells/ml and cell proliferation was monitored for seven days.  $n = 3$  independent biological replicates for K562-WT cells, and  $n = 2$  independent biological replicates for PE3-Q118R and PE3-T804N cells. Data from each biological replicate are mean  $\pm$  range from a technical triplicate. (c) Same as in (a) following successive ouabain selection. K562 cells harboring the *ATP1A1*-T804N mutation were transfected with PE3 vectors targeting *ATP1A1* (Q118R). Genomic DNA was harvested 3 days post-transfection (before selection) and cells were treated (ouabain) or not (untreated) with 100  $\mu$ M ouabain until all non-resistant cells were eliminated. (d) Same as in (b) with the addition of bulk populations of K562 cells harboring both *ATP1A1*-T804N/Q118R mutations.  $n = 2$  independent biological replicates. Data from each biological replicate are mean  $\pm$  range from a technical triplicate. (e) Western blots showing  $\alpha$ -Na<sup>+</sup>/K<sup>+</sup> ATPase subunit expression in bulk populations of ouabain-selected K562 cells. An anti- $\alpha$ -Tubulin antibody was used as a loading control.  $n = 2$  independent biological replicates performed at different times with equivalent results.

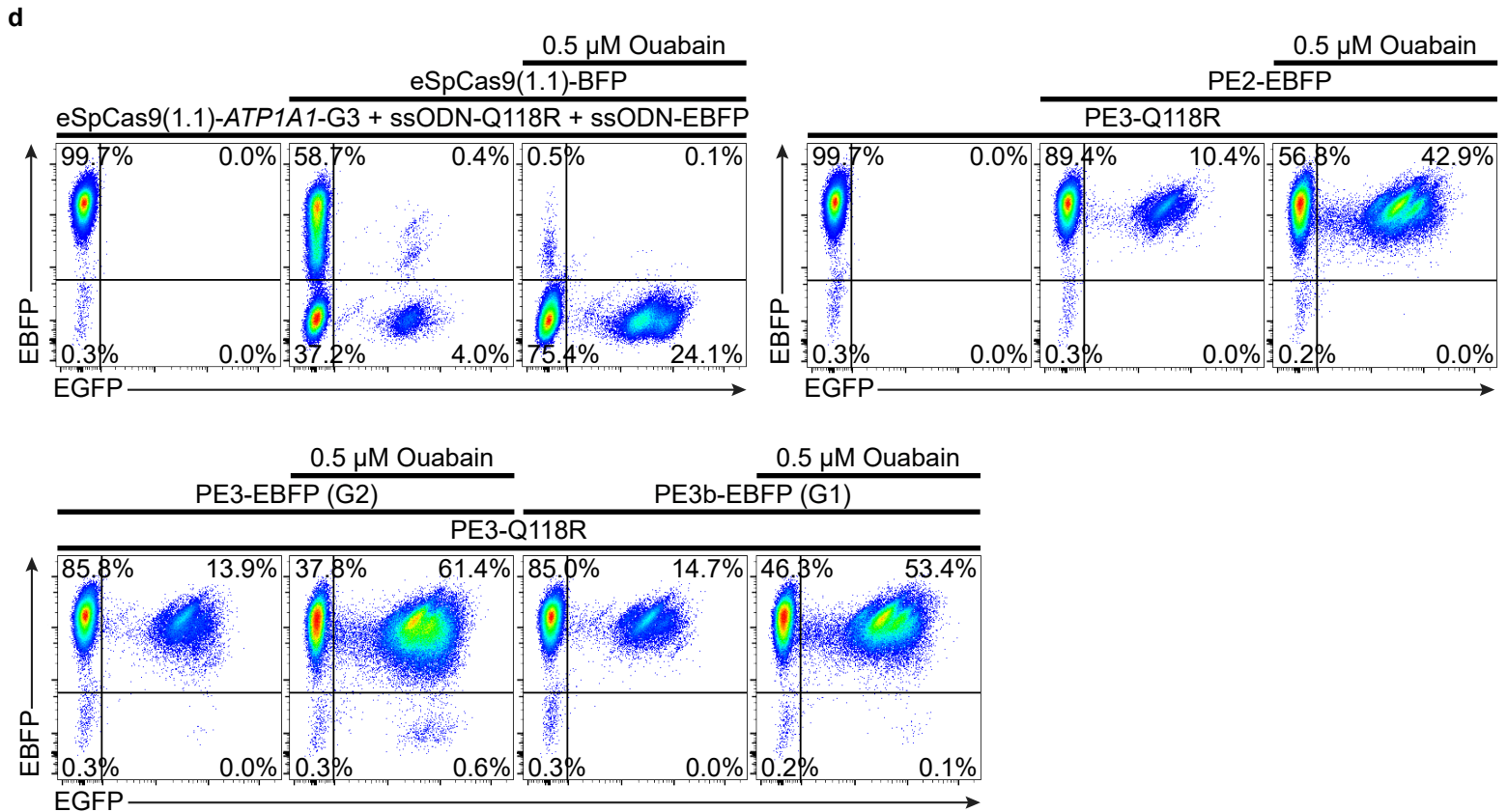
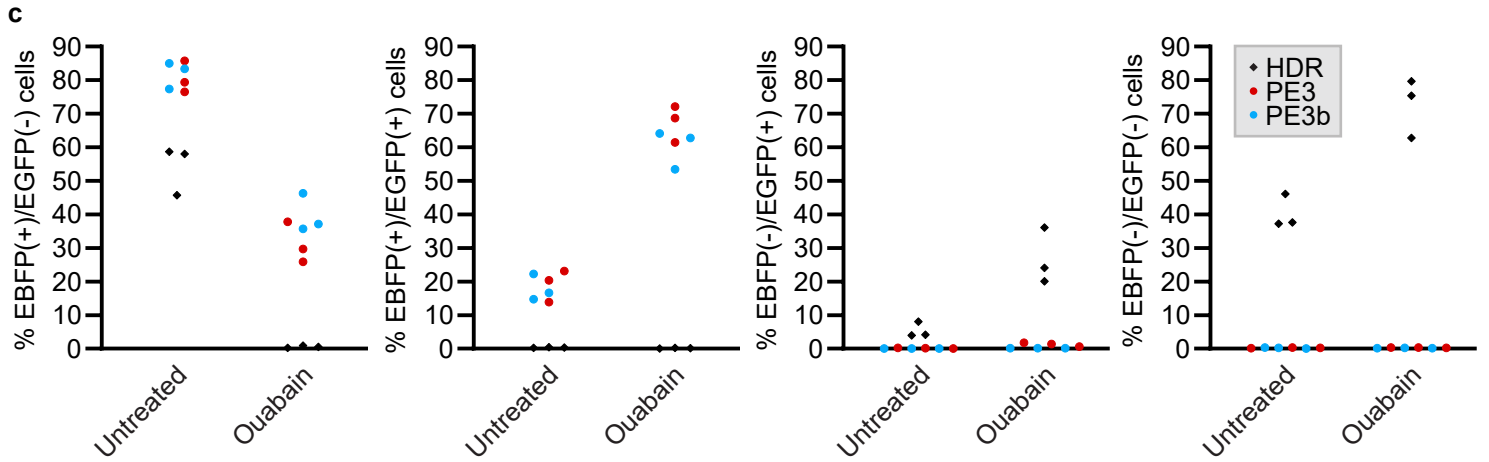
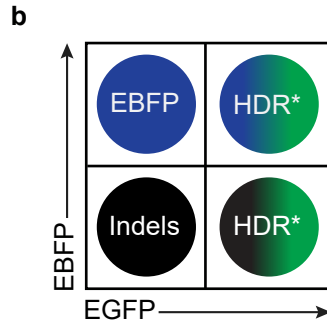
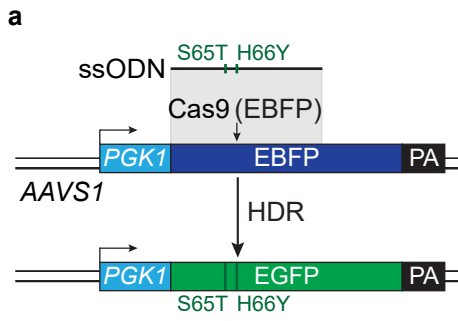




**Supplementary figure 8 (Related to Fig. 1). Robust coselection for prime editing in HeLa S3 cells.** (a) Schematic of the dual and tandem U6-driven pegRNAs and sgRNAs expression vectors along with the PE2 expression vector used to target *ATP1A1* and a gene of interest (GOI). (b) PE and small indels quantification as determined by BEAT and TIDE analysis from Sanger sequences. HeLa S3 cells were transfected with PE3 vectors targeting *ATP1A1* exon 4 (Q118R) and the indicated GOI using the standard nucleofection pulse (CN-114). Genomic DNA was harvested 3 days post-transfection (before selection) and cells were treated (ouabain) or not (untreated) with 0.5  $\mu$ M ouabain until all non-resistant cells were eliminated. (c) Same as in (b) using the high-efficiency nucleofection pulse (DS-150).  $n = 2$  independent biological replicates performed at different times with two different nucleofection pulses. Higher levels of editing were observed with the high-efficiency program, and we recommend using this nucleofection pulse for coselection in HeLa S3 cells.

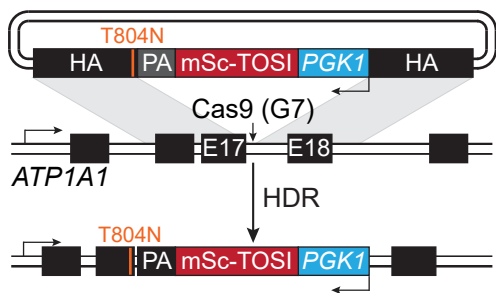


**Supplementary figure 9. Detection of PE3-mediated translocations in K562 cells** (a) Schematic representation of the chromosomal location of *ATP1A1*, *EMX1*, and *RUNX1*. (b) Nested PCR-based detection of derivative chromosome 21 (Der21). As a positive control, K562 cells were transfected with an SpCas9 nuclease-expressing vector (pX330) and dual pegRNAs- and sgRNAs-expressing vectors targeting *ATP1A1* exon 4 and *RUNX1*. Genomic DNA was harvested 3 days post-transfection. For PE3 conditions, K562 cells were transfected with PE3 vectors targeting *ATP1A1* exon 4 and *RUNX1* (see **Fig. 1**). Genomic DNA was harvested 3 days post-transfection (D3) and cells were treated (+) or not (-) with 0.5  $\mu$ M ouabain until all non-resistant cells were eliminated.  $n = 2$  independent biological replicates performed at different times. (c) Same as in (b) for derivative chromosome 2 (Der2) with pegRNAs/sgRNAs targeting *ATP1A1* exon 17 and *EMX1*. (d) Same as in (b) for derivative chromosome 21 (Der21) with pegRNAs/sgRNAs targeting *ATP1A1* exon 17 and *RUNX1*. (e) Schematic representation of a unique PE3-mediated Der2 translocation event (highlighted with \*) between *ATP1A1* and *EMX1* detected in a bulk population of K562 cells as determined by direct Sanger sequencing. (f) Schematic representation of a unique Der21 translocation event (highlighted with \*\*) between *ATP1A1* and *RUNX1* detected in a bulk population of K562 cells as determined by direct Sanger sequencing.

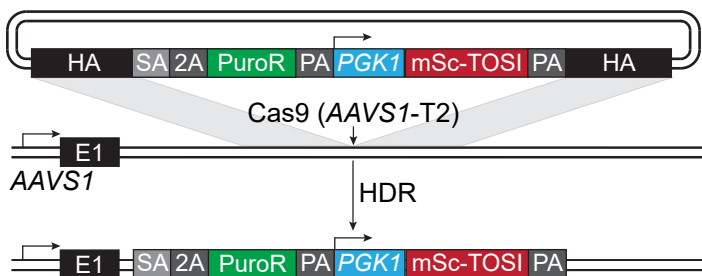


**Supplementary figure 10. Coselection for HDR or PE using an EBFP to EGFP reporter system.** (a) Schematic representation of the EBFP to EGFP reporter system via HDR-based editing using a ssODN donor. (b) Schematic of the FACS plots following HDR-based editing of the EBFP to EGFP reporter. Precise EBFP to EGFP conversion via HDR leads to the generation of EGFP(+) cells while the fluorescence signal is lost after the introduction of indels via NHEJ-based editing. \*Edited EGFP(+) cells can harbor small indels on remaining alleles. The EBFP transgene copy number of this cell line has not been determined. (c) FACS-based quantification of EBFP to EGFP conversion via HDR or PE. K562 cells stably expressing EBFP from the *AAVS1* locus were transfected with nuclease vectors and ssODN donors (HDR) or PE3/PE3b vectors targeting *ATP1A1* and EBFP. Where indicated, cells were treated with 0.5  $\mu$ M ouabain starting 3 days post-transfection until all non-resistant cells were eliminated.  $n = 3$  independent biological replicates performed at different times. (d) Representative FACS plots from the EBFP to EGFP experiments shown in (c).  $n = 3$  independent biological replicates performed at different times with equivalent results for the HDR, PE3, and PE3b conditions, and  $n = 2$  independent biological replicates for the PE2 condition.

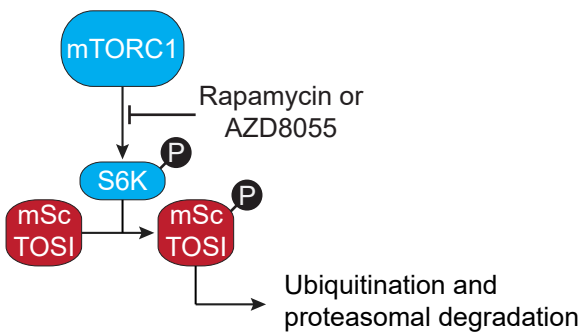
a



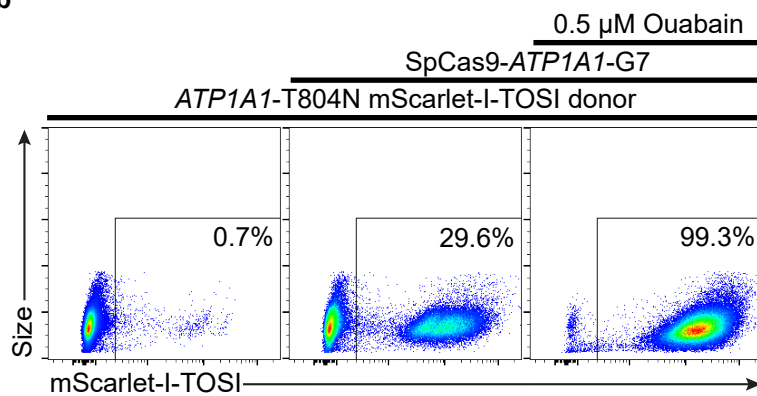
c



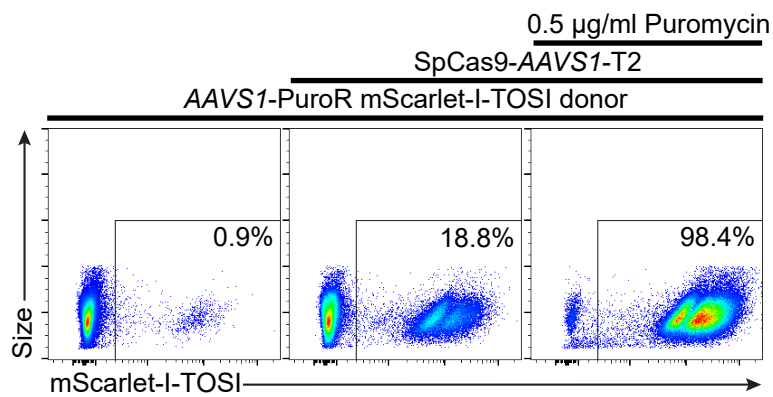
e



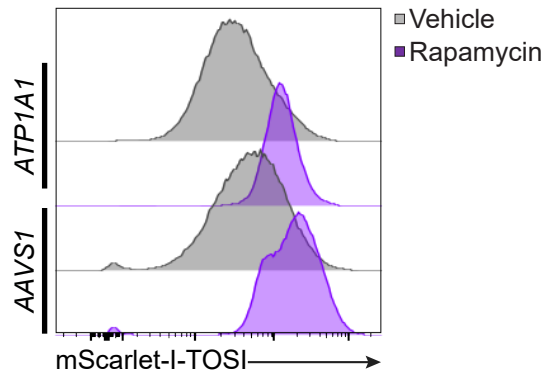
b



d

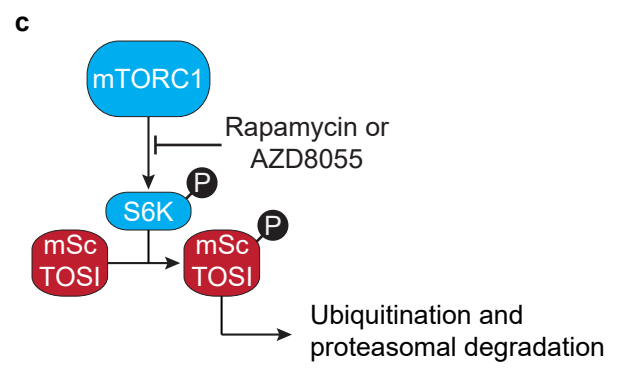
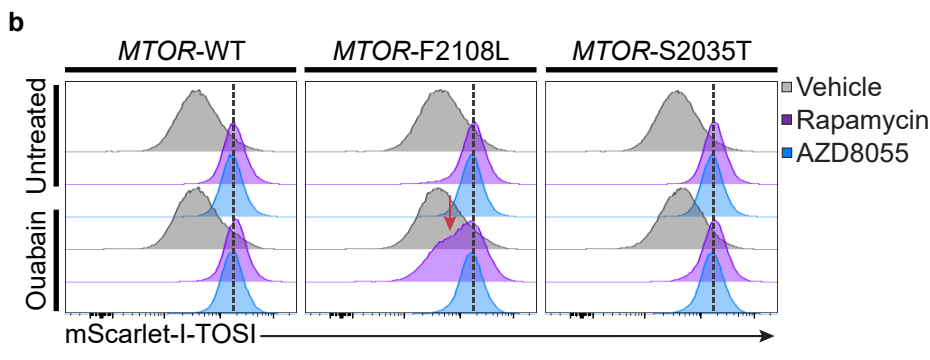
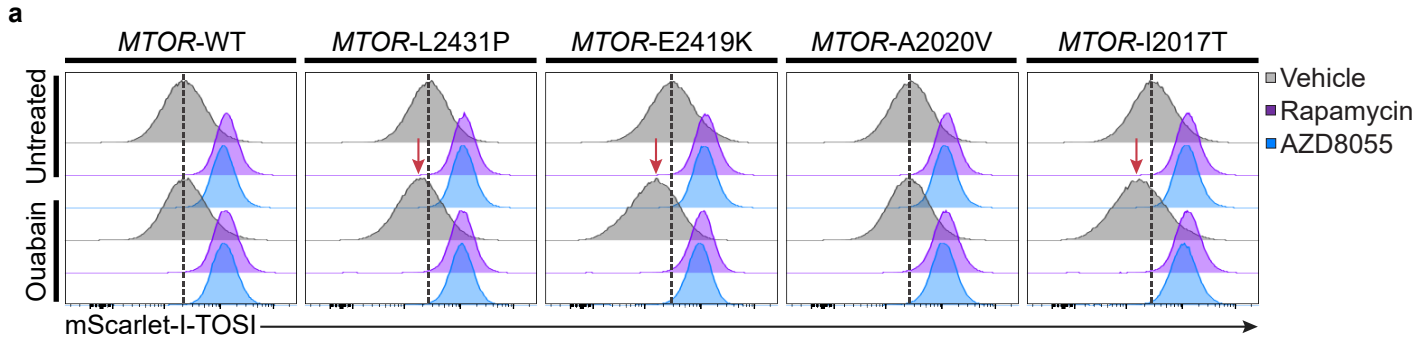


f

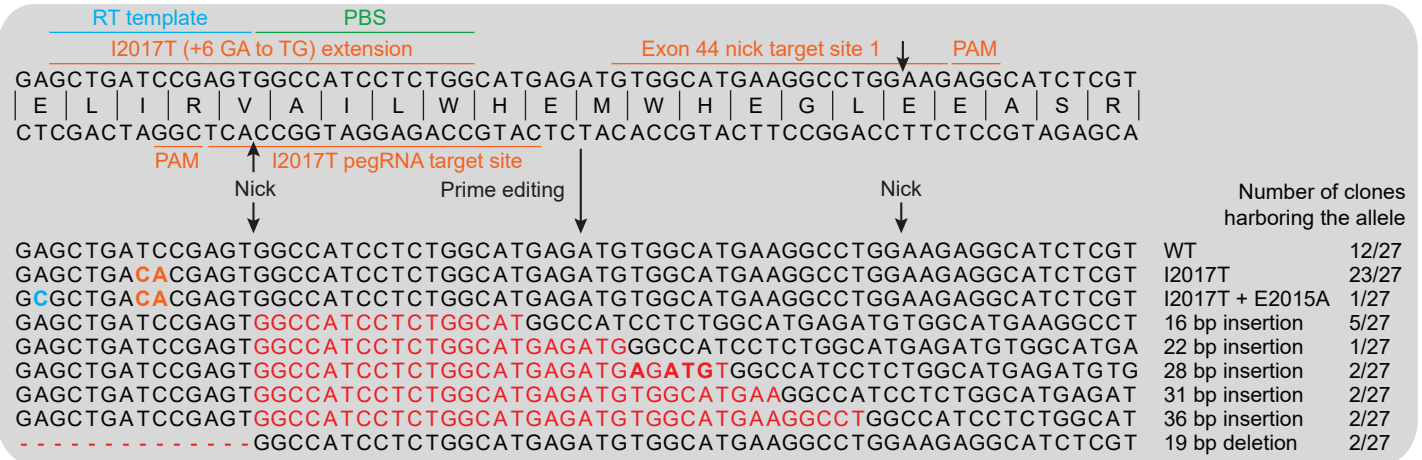
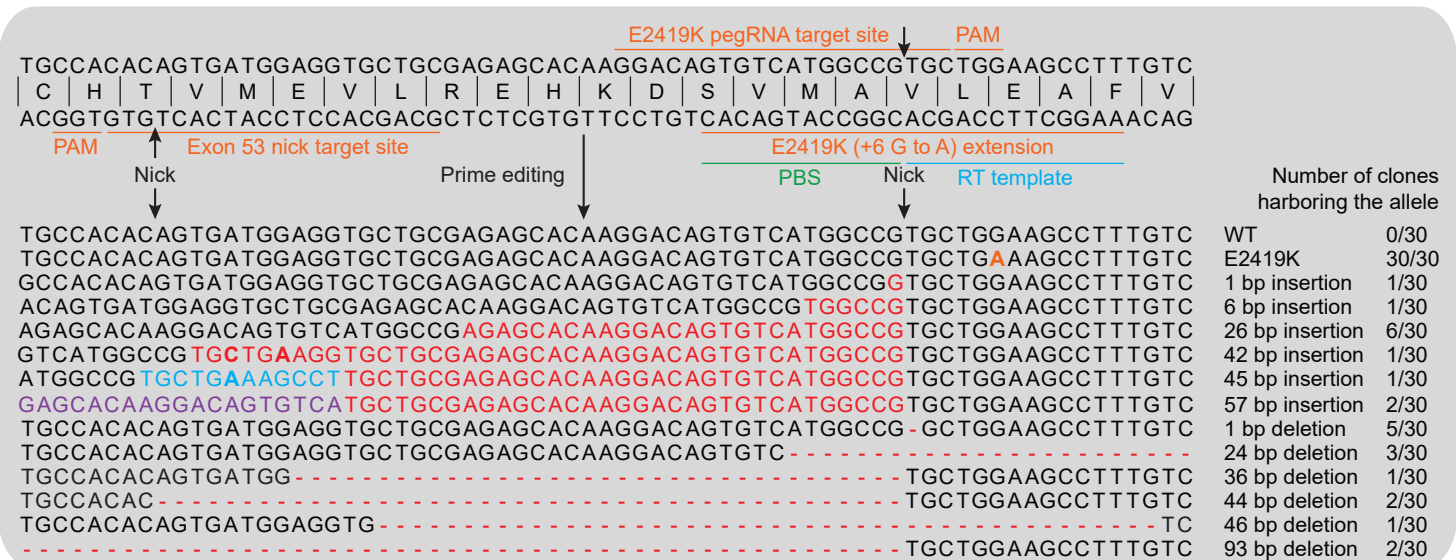


**Supplementary figure 11. *ATP1A1* as a selectable genomic harbor for targeted integration of a mTORC1 signaling reporter.** (a) Schematic representation of the targeted integration of mScarlet-I mTOR Signaling Indicator (mSc-TOSI) in antisense orientation within intron 17 of *ATP1A1*. The T804N mutation is introduced via the left homology arm (HA) and transgene expression is driven by the *PGK1* promoter. (b) FACS-based quantification of mSc-TOSI knock-in at *ATP1A1* intron 17. K562 cells were transfected with SpCas9 and the donor and treated with or without 0.5  $\mu$ M ouabain starting 3 days post-transfection until all non-resistant cells were eliminated. (c) Schematic representation of mSc-TOSI targeting to the *AAVSI* locus. (d) FACS-based quantification of mSc-TOSI knock-in at *AAVSI*. K562 cells were transfected with SpCas9 and a donor targeting *AAVSI* and treated with or without 0.5  $\mu$ g/ml puromycin starting 3 days post-transfection until all non-resistant cells were eliminated. (e) Schematic of mSc-TOSI degradation under mTORC1 signaling. (f) mSc-TOSI fluorescence intensity after stable integration at the *ATP1A1* and *AAVSI* loci in presence and absence of rapamycin. Where indicated, cells were treated with 500 nM rapamycin or vehicle control for 24 hours before FACS analysis.  $n = 1$  experiment. SA, splicing acceptor. *PGK1*, human phosphoglycerate kinase 1 promoter. PA, polyadenylation signal. HA, homology arm. E, exon.

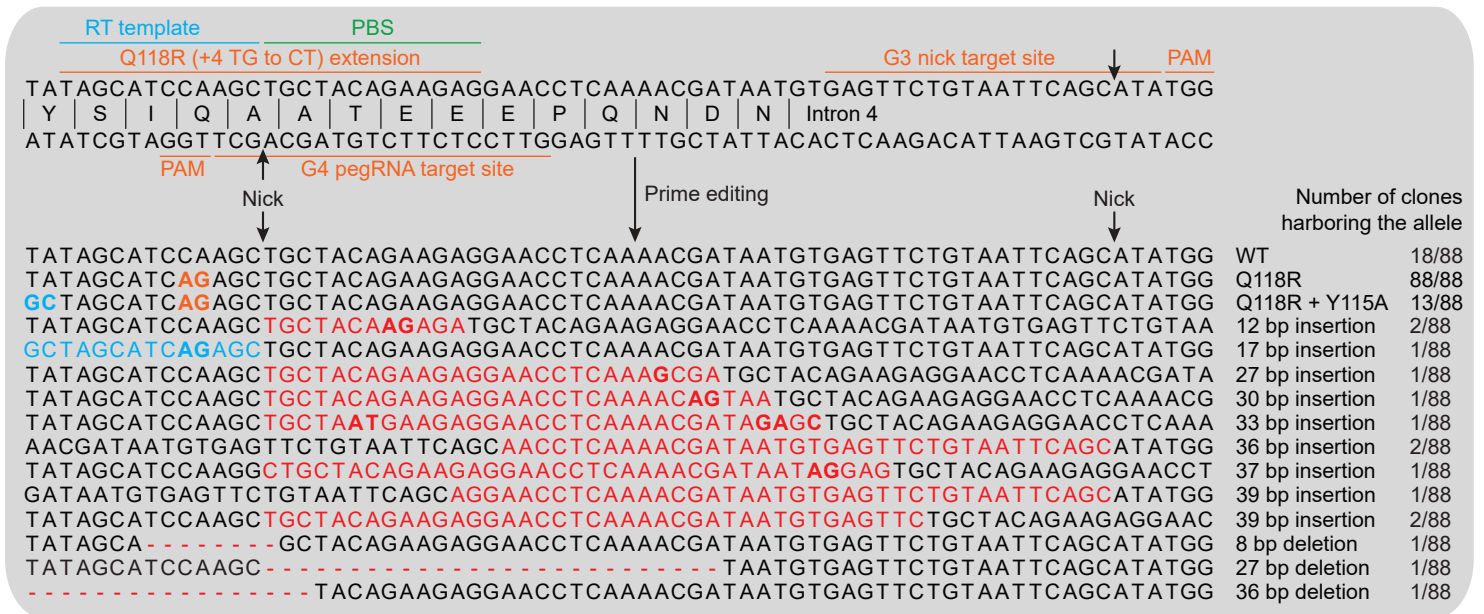




**Supplementary figure 12 (Related to Fig. 3). mSc-TOSI reporter intensity in bulk coselected populations of K562 cells.** (a) Histogram plot of mSc-TOSI intensity after coselection for *MTOR* hyperactivating mutations. As described in **Fig. 3**, K562 cells stably expressing the mSc-TOSI reporter were transfected with PE3 vectors targeting *ATP1A1* exon 4 (Q118R) and *MTOR*. Cells were treated with or without 100  $\mu$ M ouabain 3 days post-transfection until all non-resistant cells were eliminated. After coselection, cells were treated for 24 hours with 50 nM rapamycin or 50 nM AZD8055 before FACS analysis. (b) Same as in (a) with *MTOR* rapamycin-resistant mutations. Representative images are from one of two independent biological replicates performed at different times with equivalent results. (c) Schematic of mSc-TOSI degradation under mTORC1 signaling.

**a****b****c**

d



**Supplementary figure 13 (Related to Fig. 3 and Table 1). PE3-induced indels at *MTOR* and *ATP1A1* in single cell-derived clones.** (a) Schematic representation of the targeting strategy and the PE-induced insertions and deletions at *MTOR* exon 44 as determined by DECODR Sanger sequencing trace analysis. Single cell-derived K562 clones were isolated in methylcellulose-based semi-solid RPMI media supplemented with 100  $\mu$ M ouabain and genomic DNA was harvested after coselection. (b) Same as in (a) for *MTOR* exon 53. (c). Same as in (a) for *MTOR* exon 45. (d) Same as in (a) for *ATP1A1* exon 4 (Q118R) from all single cell-derived K562 clones. Nucleotide substitutions are highlighted in bold. Insertions and deletions are highlighted in red, potential RT template and pegRNA scaffold incorporations in blue, and additional small locus duplications or uncharacterized insertions are highlighted in purple.



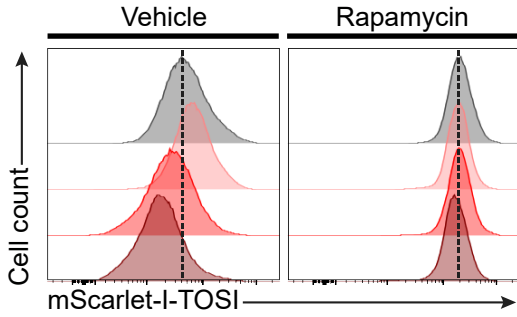


**Supplementary figure 14 (Related to Fig. 3 and Table 1). Large PE3-mediated insertions in single cell-derived clones.** (a) PCR-based genotyping of *MTOR* exon 44 from single cell-derived K562 clones harboring the *MTOR*-I2017T hyperactivating mutation.  $n = 27$  single cell-derived clones from one experiment. (b) Same as in (a) for *ATP1A1* exon 4. (c) PCR-based genotyping of *MTOR* exon 53 from single cell-derived K562 clones harboring the *MTOR*-E2419K hyperactivating mutation.  $n = 30$  single cell-derived clones from one experiment. (d) Same as in (c) for *ATP1A1* exon 4. (e) PCR-based genotyping of *MTOR* exon 45 from single cell-derived K562 clones harboring the *MTOR*-F2108L rapamycin resistance mutation.  $n = 31$  single cell-derived clones from one experiment. (f) Same as in (e) for *ATP1A1* exon 4. (g) PCR-based genotyping of *MTOR* exon 53 from single cell-derived K562 clones harboring the *MTOR*-L2431P hyperactivating mutation.  $n = 48$  single cell-derived clones from one experiment. The number of precise prime edited alleles was determined from BEAT Sanger sequencing trace analysis and small insertions and deletions were analysed with DECODR. Larger insertions are indicated, and homozygous single cell-derived clones are highlighted in bold and green. PE alleles harboring pegRNA scaffold incorporation are indicated (si). PCR products that were not sent for sequencing (*MTOR*-L2431P clones) are highlighted with a star.

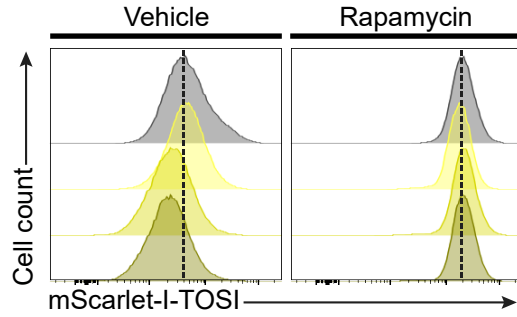
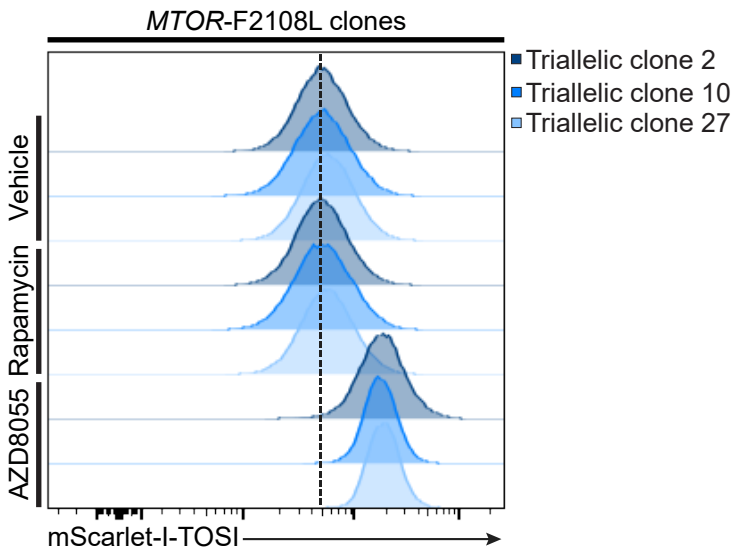
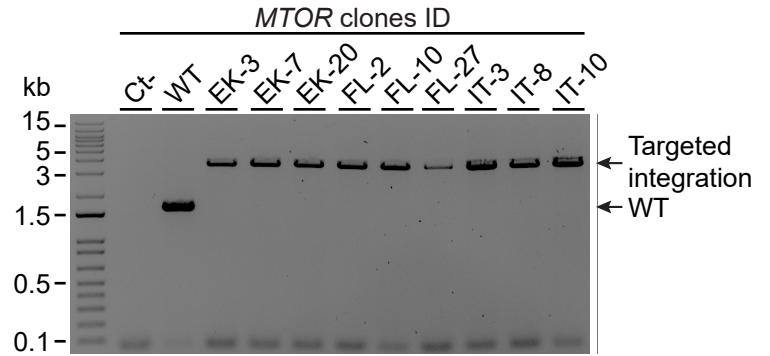


**a**

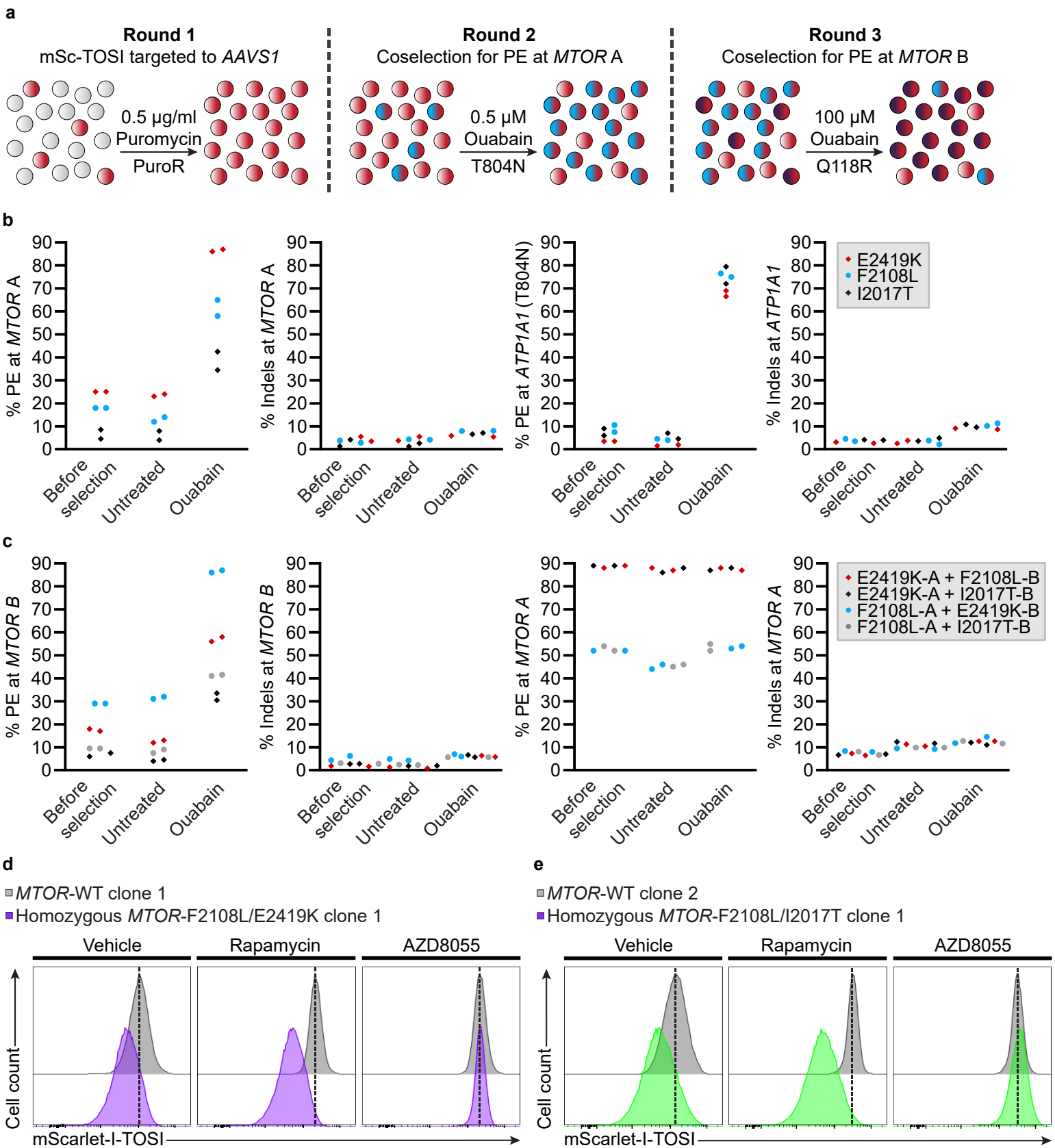
- *MTOR*-WT
- Monoallelic *MTOR*-E2419K + indels clone 7
- Biallelic *MTOR*-E2419K+ indel clone 20
- Triallelic *MTOR*-E2419K clone 3 (homozygous)



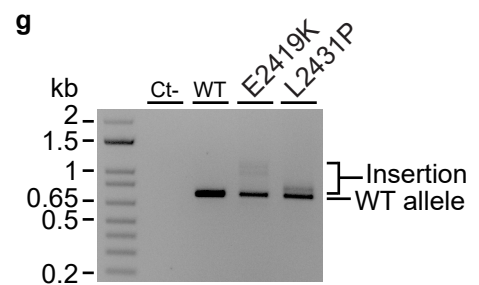
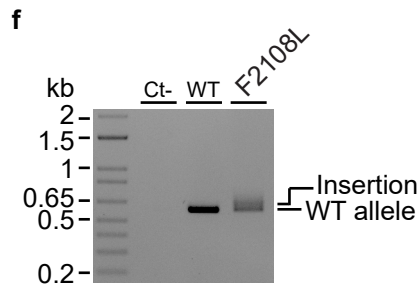
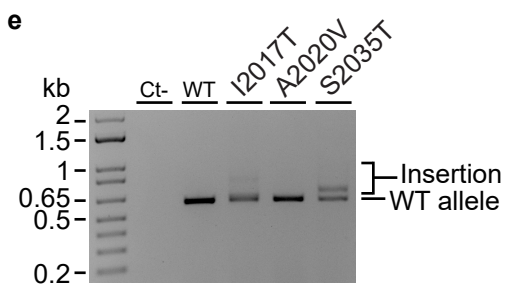
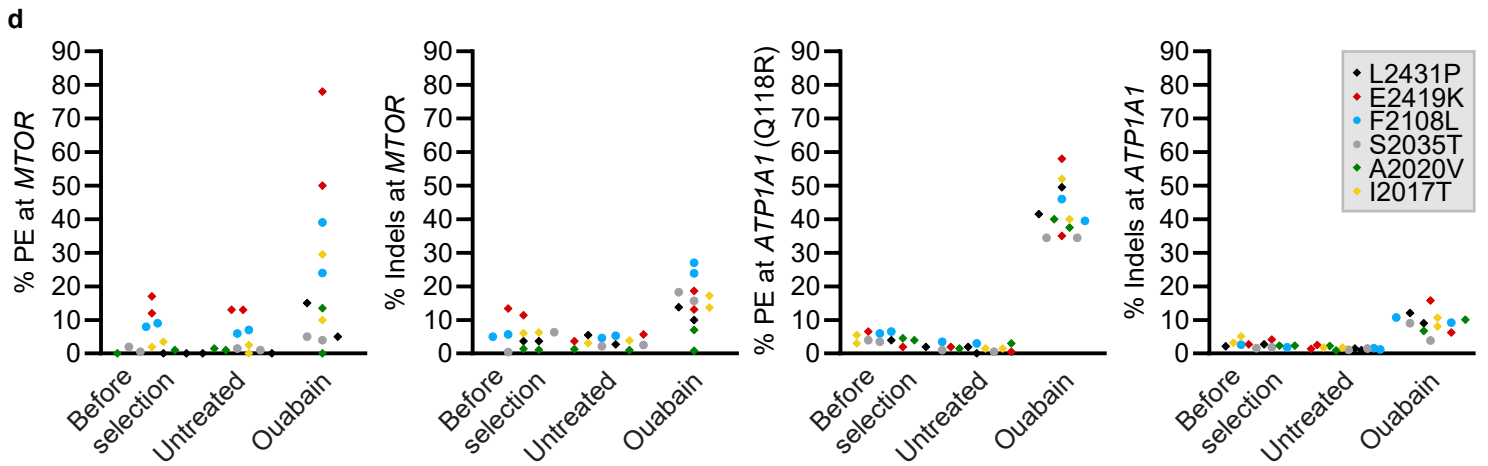
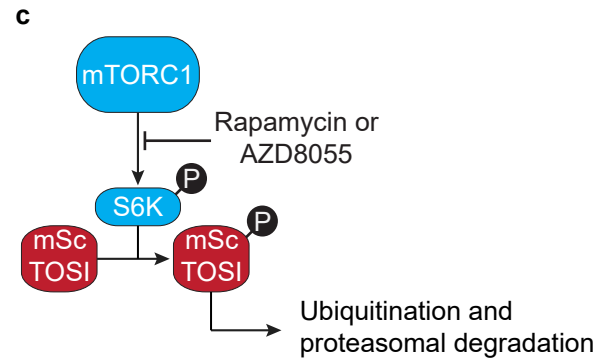
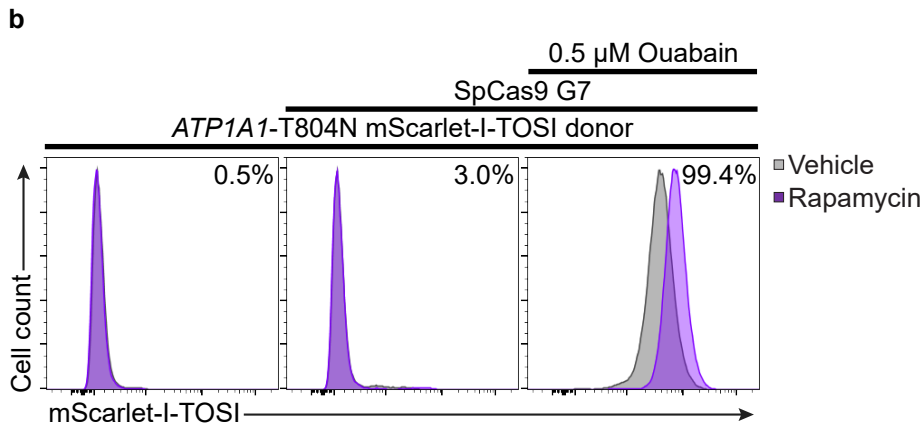
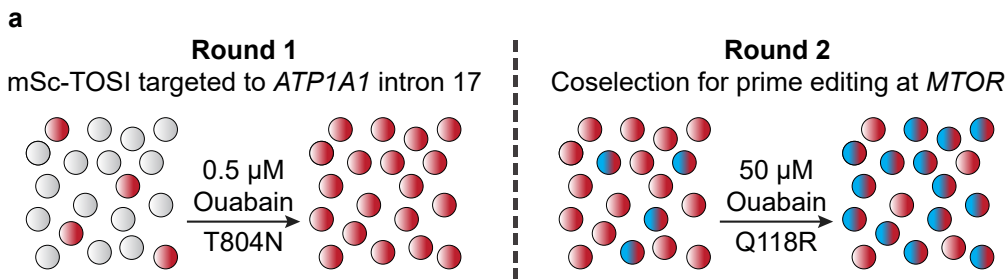
- *MTOR*-WT
- Monoallelic *MTOR*-I2017T + indels clone 10
- Biallelic *MTOR*-I2017T + indel clone 8
- Triallelic *MTOR*-I2017T clone 3 (homozygous)

**b****c**

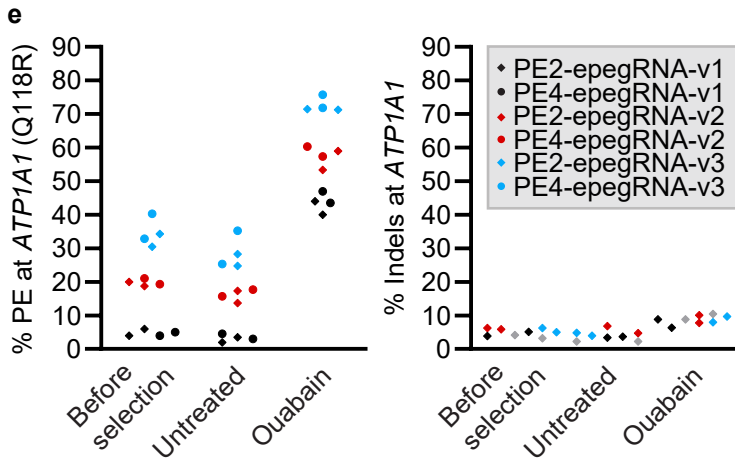
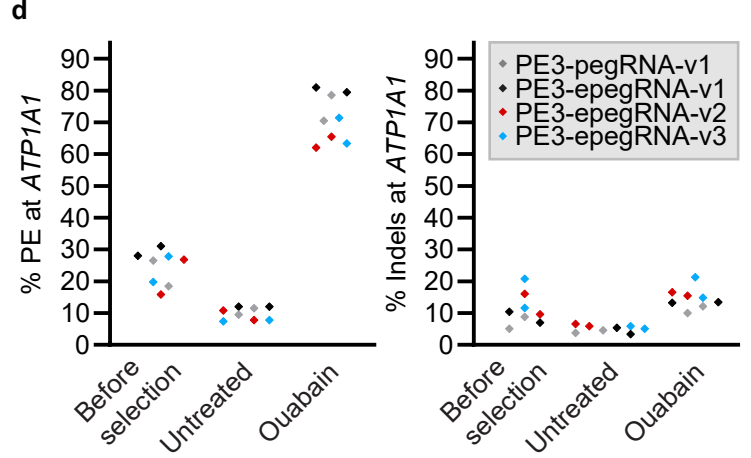
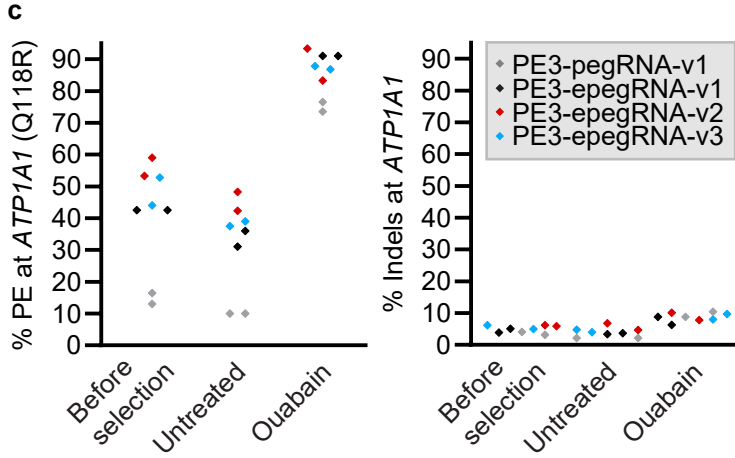
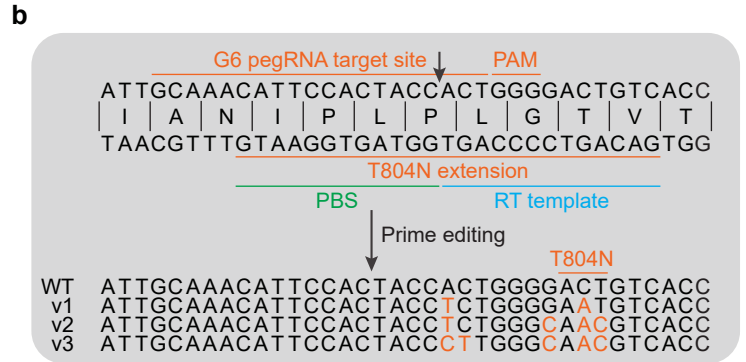
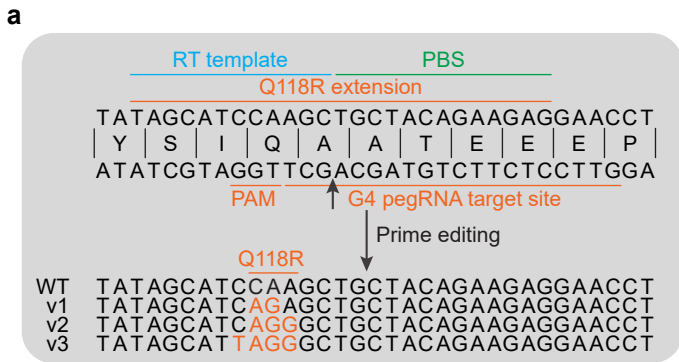
**Supplementary figure 15 (Related to Fig. 3 and Table 1). mSc-TOSI reporter intensity in single cell-derived clones harboring *MTOR* mutations.** (a) Histogram plot of mSc-TOSI intensity in monoallelic, biallelic, and triallelic (homozygous) single cell-derived K562 clones harboring *MTOR* hyperactivating mutations. (b) Same as in (a) with homozygous clones harboring the *MTOR*-F2108L rapamycin resistance mutation. After coselection, cells were treated for 24 hours with 50 nM rapamycin or 50 nM AZD8055 before FACS analysis. Representative FACS images are from one of two independent biological replicates performed at different times with equivalent results (See **Fig. 3**). (c) Out-Out PCR for mSc-TOSI knock-in detection at *ATPIA1* intron 17 in single cell-derived clones.  $n = 9$  single cell-derived clones from one experiment.



**Supplementary figure 16. Successive rounds of coselection for the isolation of double *MTOR* mutants.** (a) Schematic representation of reporter cell line engineering. K562 cells stably expressing the mSc-TOSI reporter from the *AAVSI* locus are first selected with 0.5  $\mu\text{g/ml}$  puromycin (see **Supplementary Fig. 11**). Following the first round of selection with puromycin, coselection for PE to install the first mutation at *MTOR* (*MTOR* A) is performed with 0.5  $\mu\text{M}$  ouabain. Then, a successive round of coselection for PE to install the second mutation at *MTOR* (*MTOR* B) is performed with 100  $\mu\text{M}$  ouabain. (b) PE and small indels quantification as determined by BEAT and TIDE analysis from Sanger sequencing. K562 cells stably expressing the mSc-TOSI reporter from the *AAVSI* locus were transfected with PE3 vectors targeting *ATP1A1* exon 17 (T804N) and *MTOR* A. Genomic DNA was harvested 3 days post-transfection (before selection) and cells were treated (ouabain) or not (untreated) with 0.5  $\mu\text{M}$  ouabain until all non-resistant cells were eliminated.  $n = 2$  independent biological replicates performed at different times. (c) Same as in (b) for a successive round of coselection for PE at *MTOR* B with K562 cells harboring the *ATP1A1*-T804N and the indicated *MTOR* A mutation. Successive coselection was performed with 100  $\mu\text{M}$  ouabain until all non-resistant cells were eliminated.  $n = 2$  independent biological replicates performed at different times. (d) Histogram plot of mSc-TOSI intensity in a homozygous single cell-derived K562 clone harboring the *MTOR*-F2108L rapamycin resistance mutation and the *MTOR*-E2419K hyperactivating mutation. (e) Same as in (d) with a homozygous clone harboring the *MTOR*-F2108L rapamycin resistance mutation and the *MTOR*-I2017T hyperactivating mutation. Where indicated, cells were treated for 24 hours with 50 nM rapamycin or 50 nM AZD8055 before FACS analysis. Representative images are from one of two independent biological replicates performed at different times with equivalent results (see **Fig. 3**).



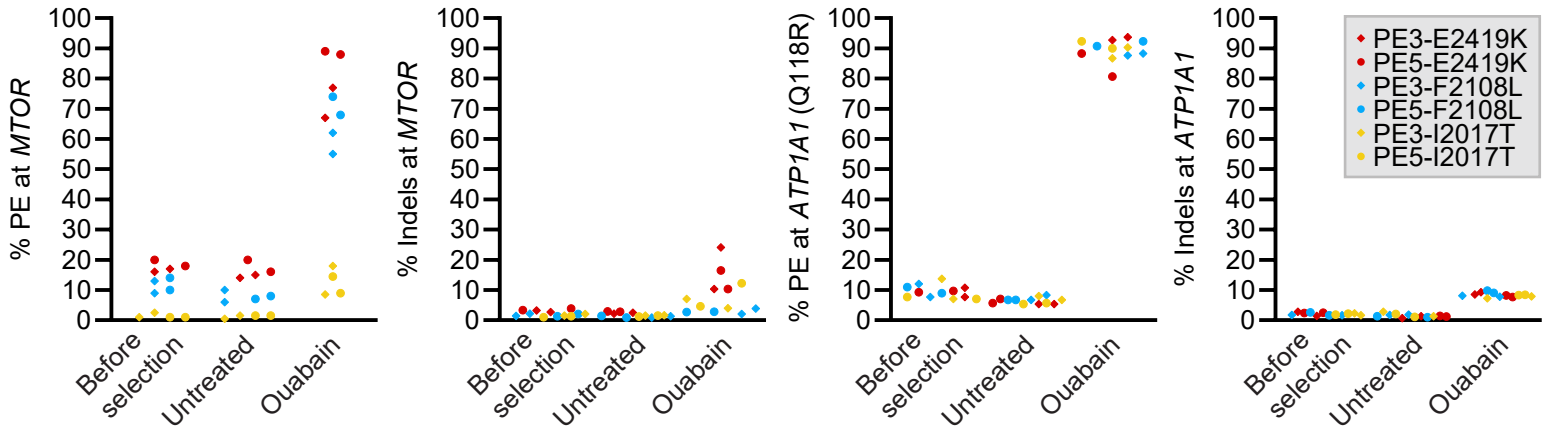
**Supplementary figure 17 (Related to Fig. 3). Sequential mSc-TOSI knock-in and coselection for prime editing at *MTOR* in HeLa S3 cells.** (a) Schematic representation of reporter cell line engineering. HeLa S3 cells stably expressing the mSc-TOSI reporter from *ATP1A1* intron 17 are first selected with 0.5  $\mu$ M ouabain. Then, coselection for PE to insert the indicated mutations at *MTOR* is performed with 50  $\mu$ M ouabain. (b) FACS-based quantification of mSc-TOSI knock-in at *ATP1A1* intron 17. HeLa S3 cells were transfected with SpCas9 and a donor targeting *ATP1A1* and treated with or without 0.5  $\mu$ M ouabain 3 days post-transfection until all non-resistant cells were eliminated. Where indicated, cells were treated for 24 hours with 500 nM rapamycin before FACS analysis. Representative FACS images are from one of two independent biological replicates performed at different times with equivalent results. (c) Schematic of mSc-TOSI degradation under mTORC1 signaling. In these cells the difference in fluorescence observed by FACS-based analysis was too minimal between the on and off states (+/- rapamycin) to monitor the impact of PE-induced mutations. (d) PE and small indels quantification as determined by BEAT and TIDE analysis from Sanger sequences. HeLa S3 cells stably expressing the mSc-TOSI reporter were transfected with PE3 vectors targeting *ATP1A1* exon 4 (Q118R) and *MTOR*. Genomic DNA was harvested 3 days post-transfection (before selection) and cells were treated (ouabain) or not (untreated) with 50  $\mu$ M ouabain until all non-resistant cells were eliminated.  $n = 2$  independent biological replicates performed at different times. (e) PCR-based detection of large PE-mediated insertions at *MTOR* exon 44 in bulk coselected populations of HeLa S3 cells.  $n = 2$  independent biological replicates performed at different times. (f) Same as in (e) at *MTOR* exon 45. (g) Same as in (e) at *MTOR* exon 53.



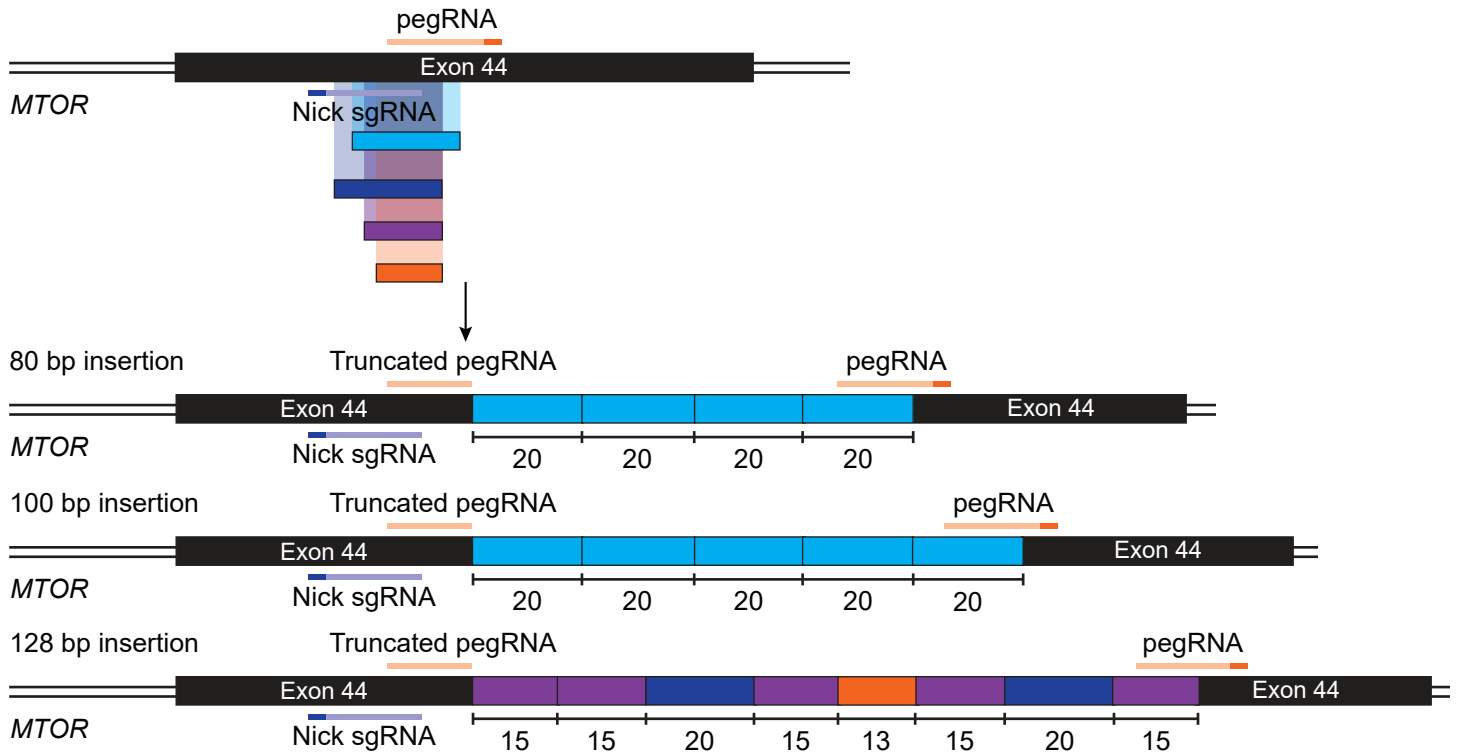
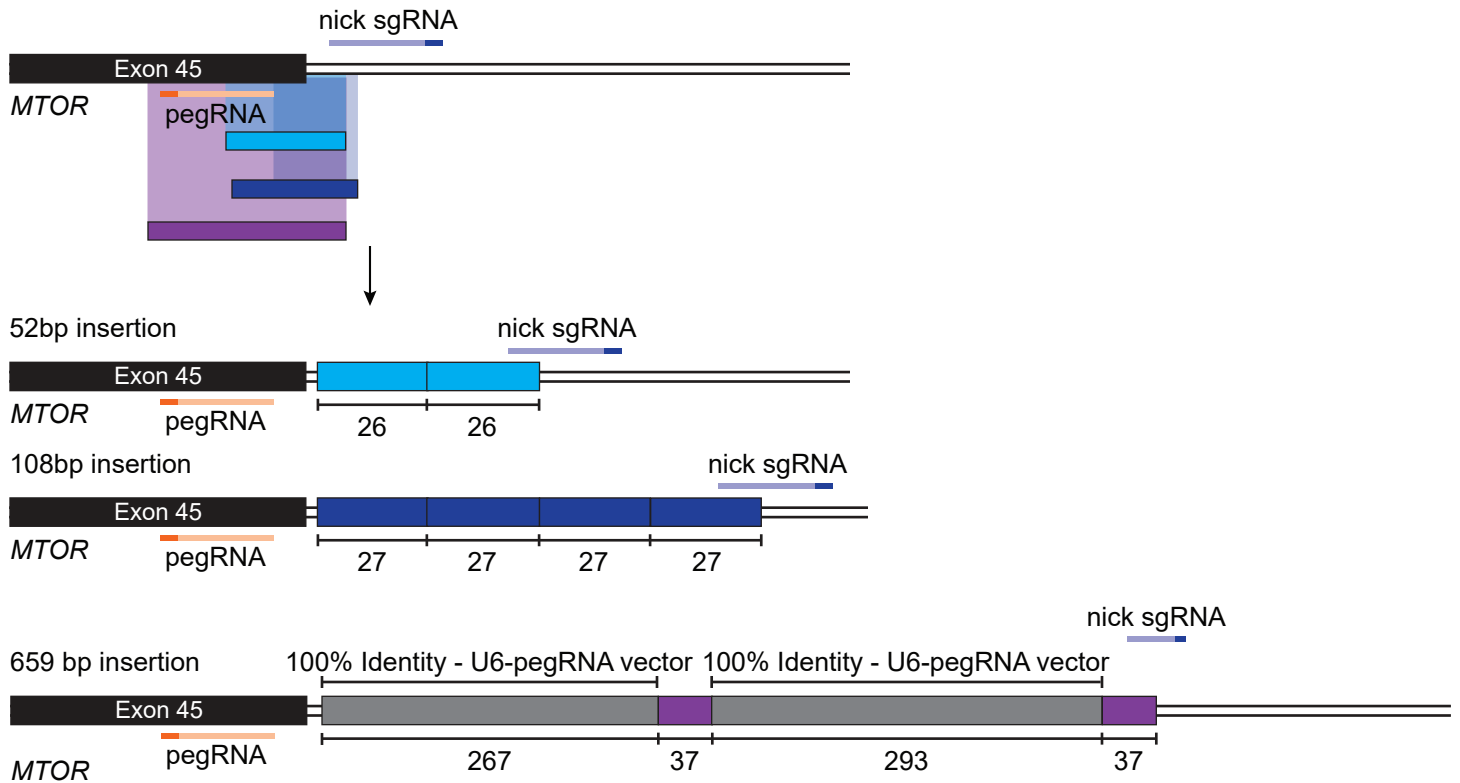
**Supplementary figure 18. Engineered pegRNAs (epegRNAs) with MMR-evading mutations enhance prime editing at *ATP1A1*.** (a) Schematic representation of the SpCas9 target site and the reverse transcriptase (RT) template used to install the Q118R mutation at *ATP1A1* exon 4 to induce cellular resistance to ouabain. New epegRNA versions harboring additional MMR-evading mutations are shown. (b) Schematic representation of the SpCas9 target site and the reverse transcriptase (RT) template used to install the T804N mutation at *ATP1A1* exon 17 to induce cellular resistance to ouabain. New epegRNA versions harboring additional MMR-evading mutations are shown. (c) PE and small indels quantification at *ATP1A1* exon 4 (Q118R) as determined by BEAT and TIDE analysis from Sanger sequences. K562 cells were transfected with PE3max vectors and genomic DNA was harvested 3 days post-transfection (before selection) and cells were treated (ouabain) or not (untreated) with 0.5  $\mu$ M ouabain for 10 days starting 3 days post-transfection.  $n = 2$  independent biological replicates performed at different times. (d) Same as in (c) at *ATP1A1* exon 17 (T804N). (e) Same as in (c), but K562 cells were transfected with PEmax (PE2) or PEmax-2A-hMLH1dn (PE4) and pegRNA vectors without an additional nick sgRNA.



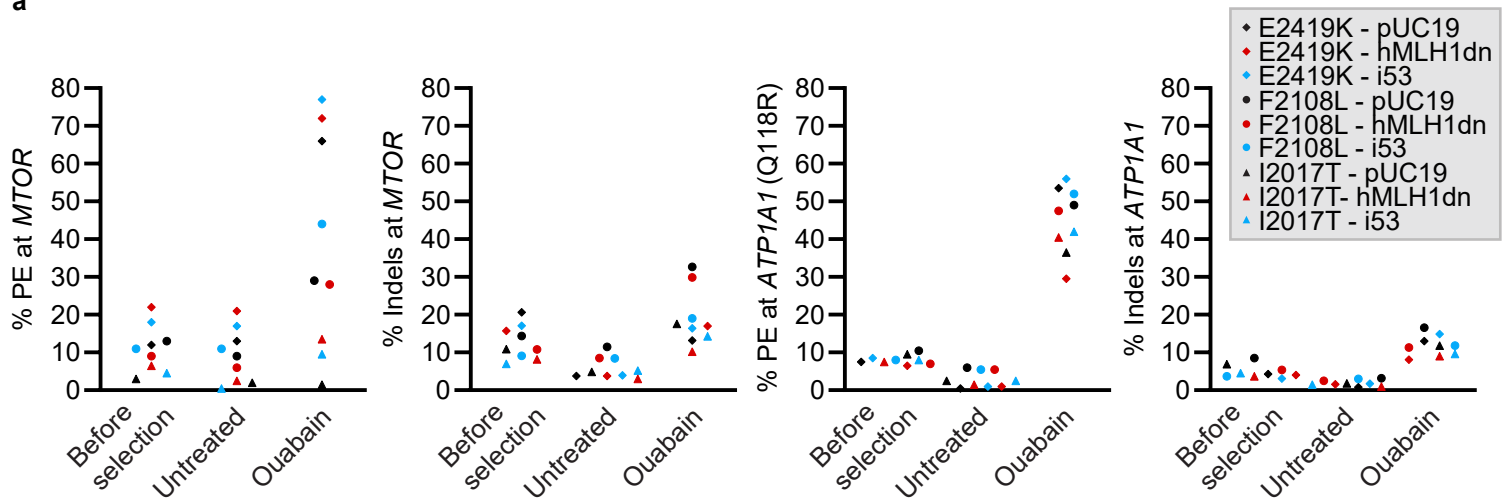
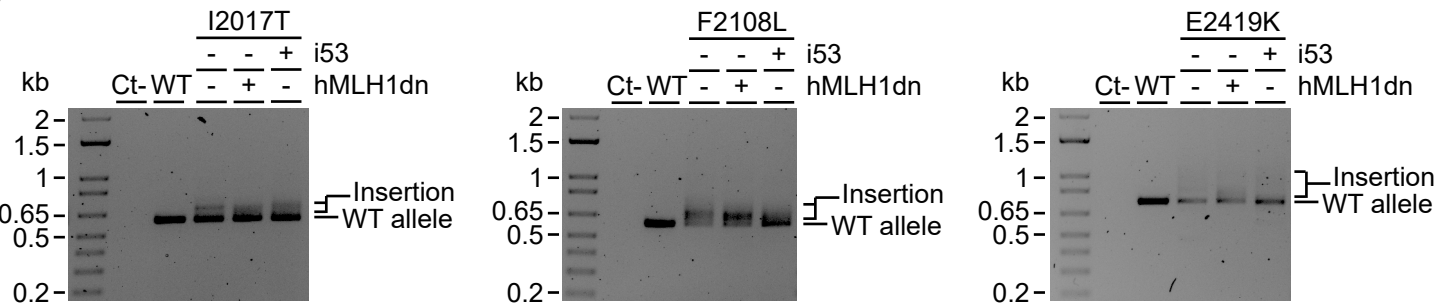
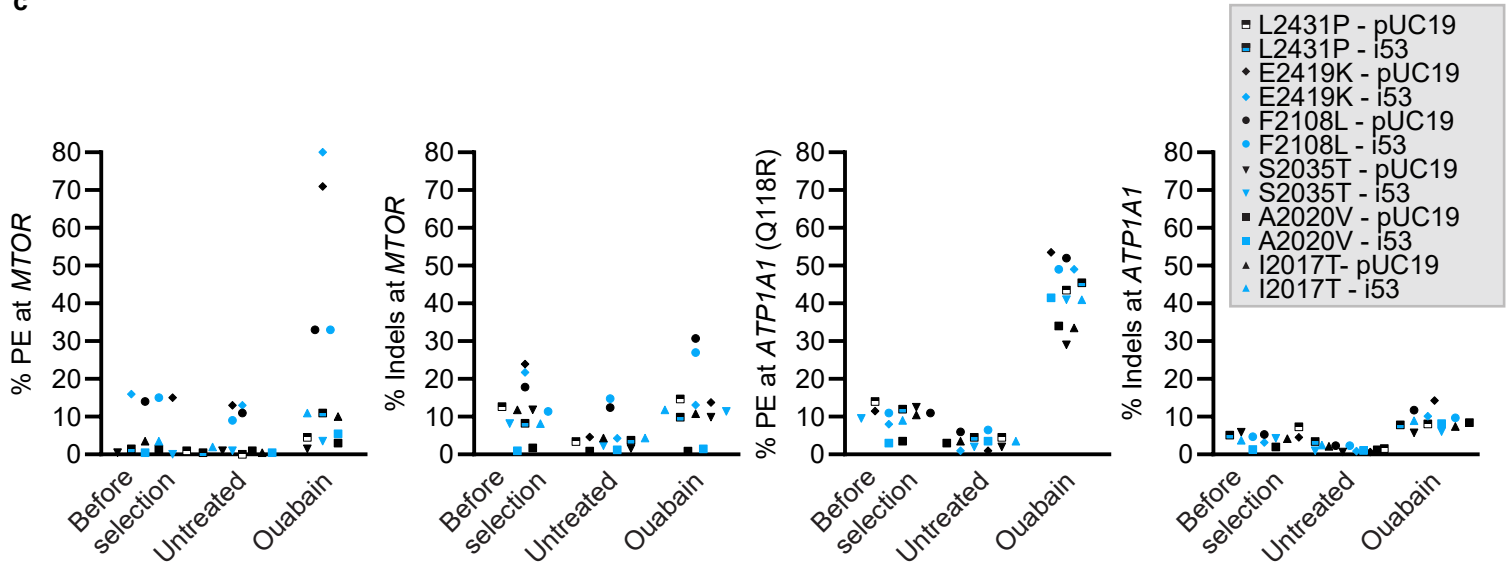
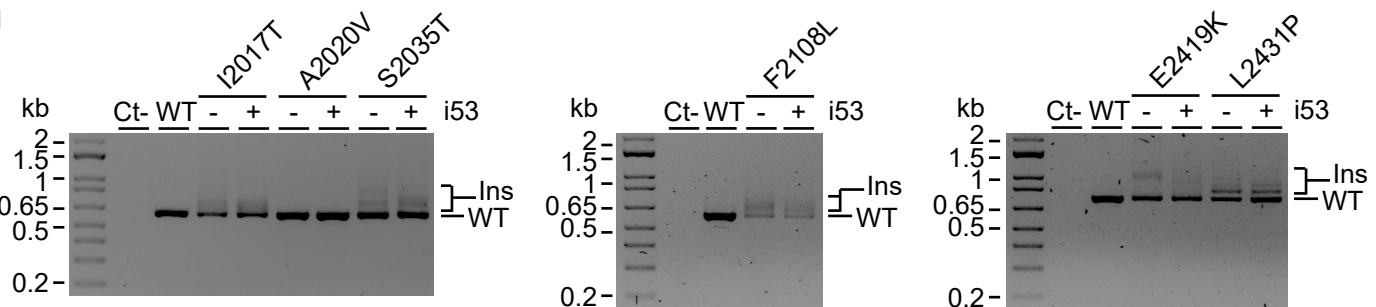
**a**



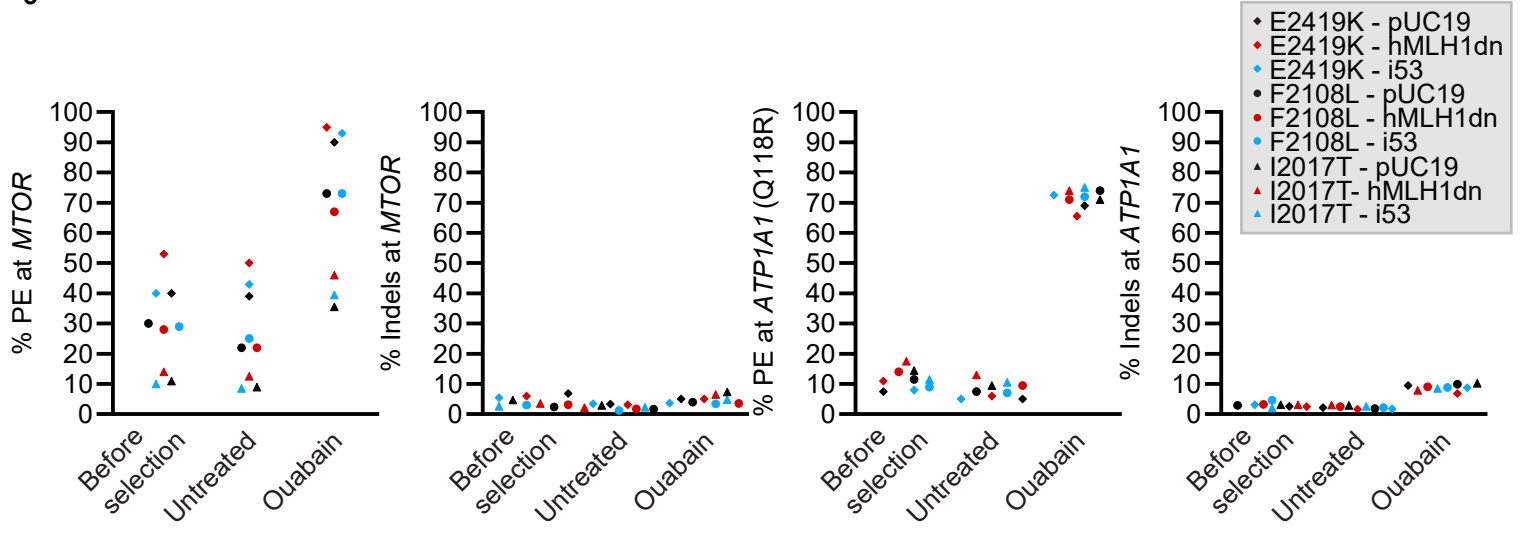
**Supplementary figure 19 (Related to Fig. 3). Robust coselection for prime editing at *MTOR* in U2OS cells with engineered pegRNAs (epegRNAs).** (a) PE and small indels quantification as determined by BEAT and TIDE analysis from Sanger sequences. U2OS cells were transfected with PE3max-epegRNA vectors targeting *ATP1A1* exon 4 (epegRNA-Q118R\_v2) and *MTOR*. Genomic DNA was harvested 3 days post-transfection (before selection) and cells were treated (ouabain) or not (untreated) with 0.5  $\mu$ M ouabain until all non-resistant cells were eliminated.  $n = 2$  independent biological replicates performed at different times.

**a**Large insertions from bulk HeLa *MTOR*-S2035T population**b**Large insertions from bulk HeLa *MTOR*-F2108L population

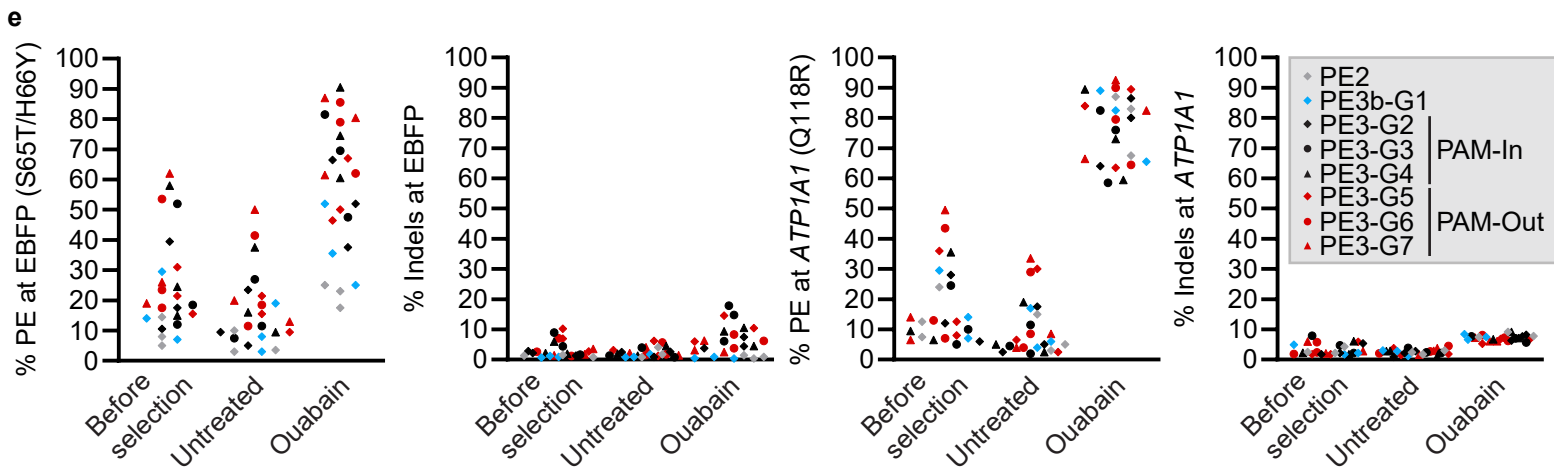
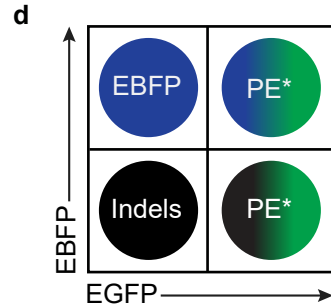
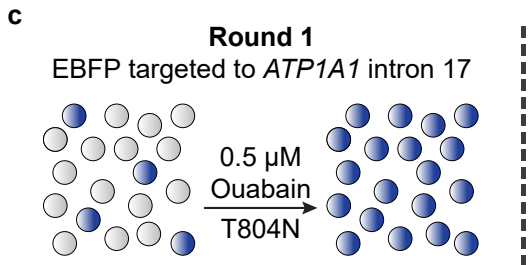
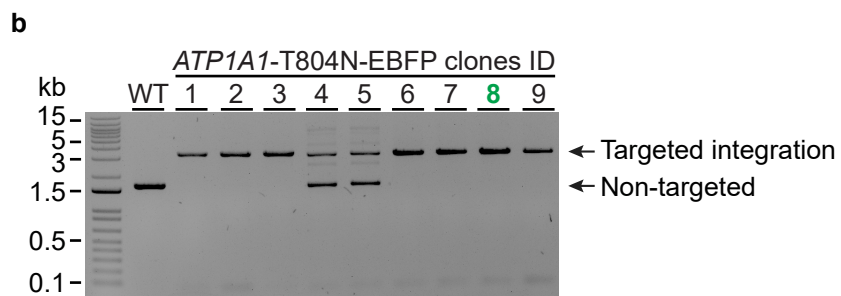
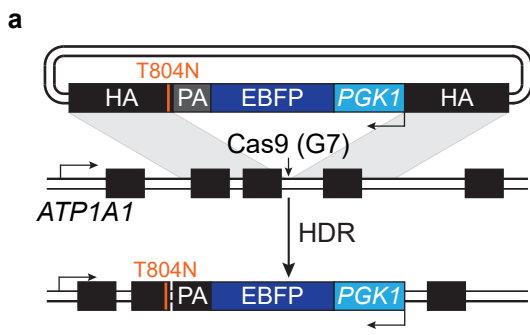
**Supplementary figure 20 (Related to Supplementary Fig. 17). Characterization of large PE3-mediated insertions in bulk populations of HeLa S3 cells.** (a) Schematic representation of the large insertions observed in HeLa S3 cells following coselection for PE at *MTOR* exon 44 for the installation of the *MTOR*-S2035T mutation. As described in **Supplementary Fig. 17**, HeLa S3 cells stably expressing the mSc-TOSI reporter were transfected with PE3 vectors targeting *ATPIA1* exon 4 (Q118R) and *MTOR*. Genomic DNA was harvested after ouabain coselection. TOPO cloning and Sanger sequencing were performed to characterize the large insertion. (b) Same as in (a) following coselection for PE at *MTOR* exon 45 for the installation of the *MTOR*-F2108L mutation.

**a****b****c****d**

e

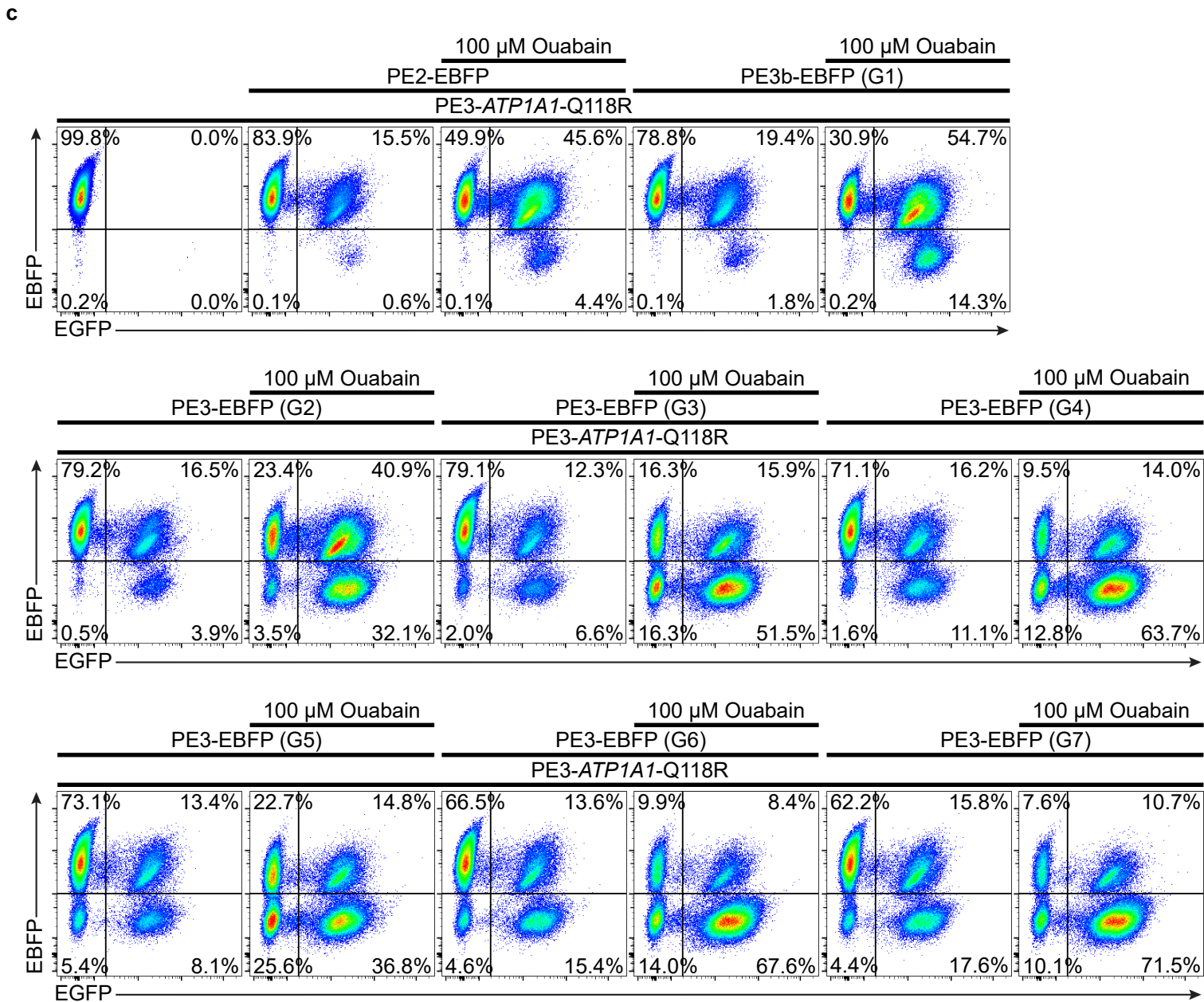
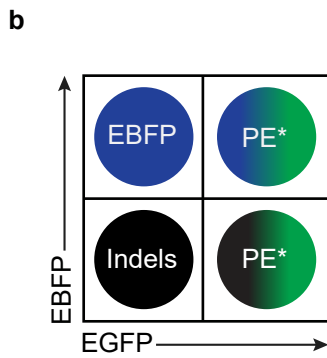
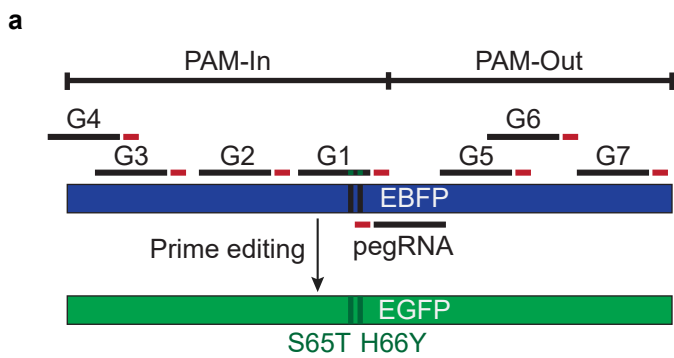


**Supplementary figure 21. Assessing the impact of 53BP1 inhibition on large PE-mediated insertions.** (a) PE and small indels quantification as determined by BEAT and TIDE analysis from Sanger sequences. HeLa S3 cells stably expressing the mSc-TOSI reporter were transfected with PE3max vectors targeting *ATP1A1* exon 4 (Q118R) and *MTOR*, and a vector expressing either hMLH1dn or i53. An empty pUC19 vector was used as a control to normalize DNA concentration in all transfections. Genomic DNA was harvested 3 days post-transfection (before selection) and cells were treated (ouabain) or not (untreated) with 50  $\mu$ M ouabain until all non-resistant cells were eliminated. (b) PCR-based detection of large PE-mediated insertions at *MTOR* exon 44, 45, and 53 in bulk coselected populations of HeLa S3 cells.  $n = 1$  experiment. (c) Experiment replicated as described in (a) using additional pegRNA/sgRNA pairs. (d) Same as in (b) with bulk populations of HeLa S3 cells from (c).  $n = 1$  experiment. (e) PE and small indels quantification as determined by BEAT and TIDE analysis from Sanger sequences. K562 cells were transfected with PE3max vectors targeting *ATP1A1* exon 4 (Q118R) and *MTOR*, and a vector expressing either hMLH1dn or i53. An empty pUC19 vector was used as a control to normalize DNA concentration in all transfections. Genomic DNA was harvested 3 days post-transfection (before selection) and cells were treated (ouabain) or not (untreated) with 0.5  $\mu$ M ouabain until all non-resistant cells were eliminated.  $n = 1$  experiment.



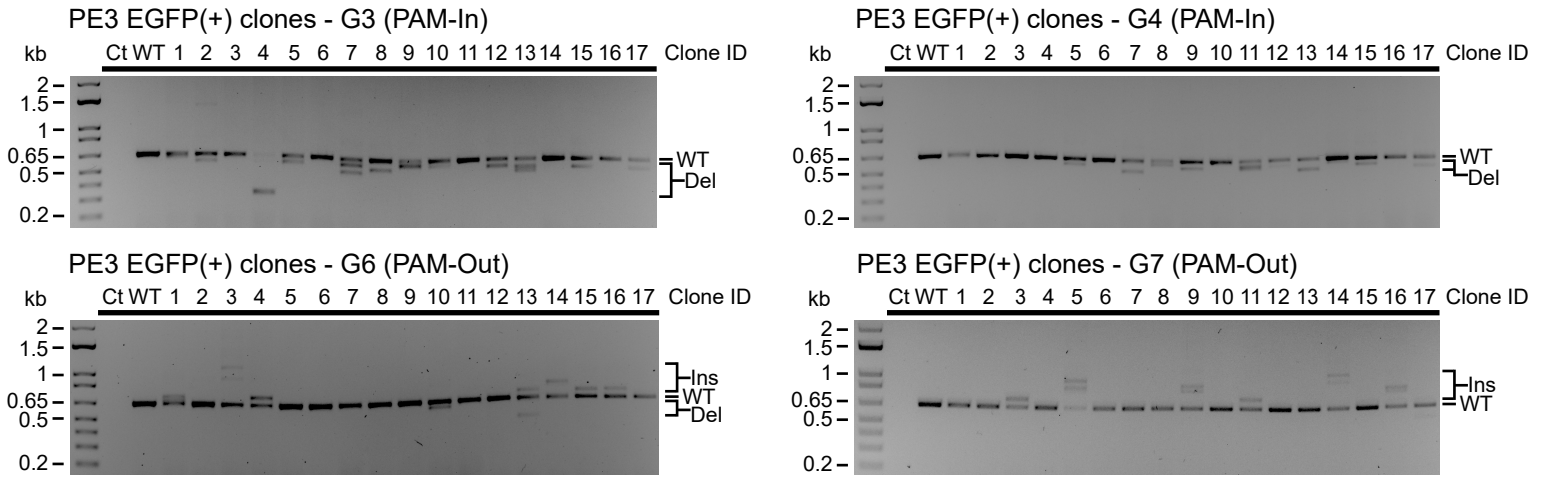


**Supplementary figure 22 (Related to Fig. 6). Assessing the impact of complementary-strand nick locations on prime editing outcomes.** (a) Schematic of targeted EBFP integration at *ATP1A1* intron 17. (b) Out-Out PCR for EBFP knock-in detection at *ATP1A1* intron 17 in single cell-derived K562 clones. The *ATP1A1*-T804N-EBFP clone that was used during this study (clone 8) is highlighted in bold and green. (c) Schematic representation of reporter cell line engineering. K562 cells stably expressing the EBFP reporter from *ATP1A1* intron 17 are first selected with 0.5  $\mu$ M ouabain. Then, coselection for EBFP to EGFP conversion via PE is performed with 100  $\mu$ M ouabain. (d) Schematic of the FACS-based quantification of EBFP to EGFP conversion via PE. In K562 cells homozygous for EBFP integration at *ATP1A1* (triallelic), FACS-based analysis reports PE outcomes indirectly; (i) EBFP(+)/EGFP(+) cells result from monoallelic or biallelic PE, (ii) EBFP(-)/EGFP(+) cells are generated by either triallelic PE or combinations of mono- and biallelic PE along with indels\*, (iii) EBFP(-)/EGFP(-) occur from indels on the three copies of the reporter. Indels are defined broadly in this context as any edits that inactivates the reporter. (e) PE and small indels quantification as determined by BEAT and TIDE analysis from Sanger sequencing. K562 cells stably expressing the EBFP reporter were transfected with PE3max vectors targeting *ATP1A1* exon 4 (pegRNA-Q118R\_v1) and EBFP (epegRNA). Genomic DNA was harvested 3 days post-transfection (before selection) and cells were treated (ouabain) or not (untreated) with 100  $\mu$ M ouabain until all non-resistant cells were eliminated.  $n = 3$  independent biological replicates performed at different times. *PGKI*, human phosphoglycerate kinase 1 promoter. PA, polyadenylation signal. HA, homology arm.

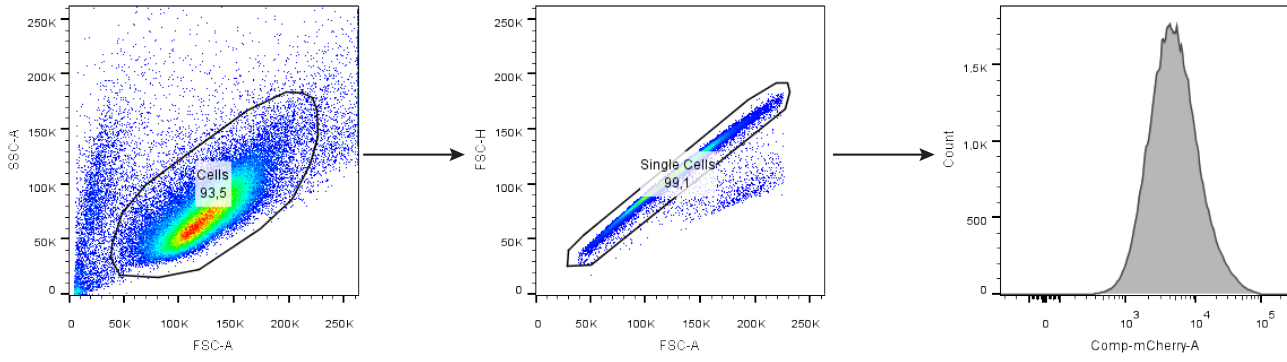
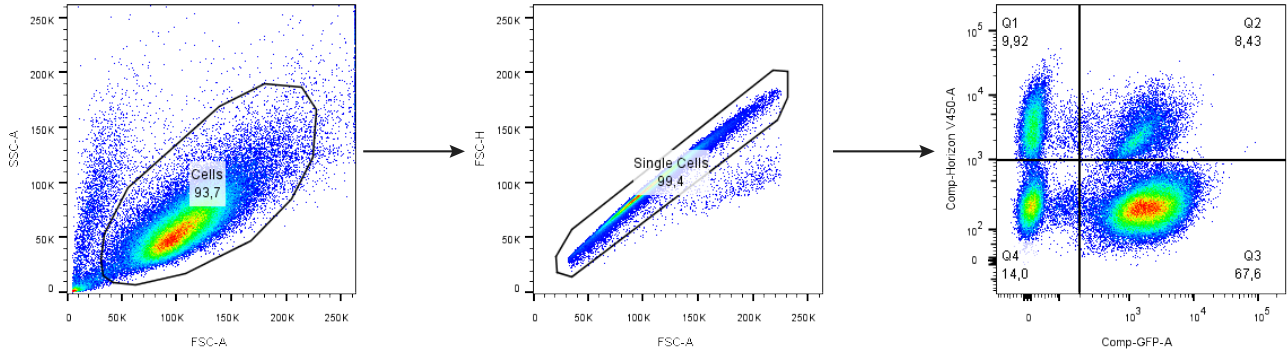


**Supplementary figure 23 (Related to Fig. 6). Representative FACS plots for EBFP to EGFP conversion.** (a) Schematic representation of the EBFP to EGFP reporter system using different nick sgRNAs with PAMs facing outwards (PAM-Out) or inwards (PAM-In) towards the pegRNA. (b) Schematic of the FACS-based quantification of EBFP to EGFP conversion via PE. In K562 cells homozygous for EBFP integration at *ATP1A1* (trialelic), FACS-based analysis reports PE outcomes indirectly; (i) EBFP(+)/EGFP(+) cells result from monoallelic or biallelic PE, (ii) EBFP(-)/EGFP(+) cells are generated by either triallelic PE or combinations of mono- and biallelic PE along with indels\*, (iii) EBFP(-)/EGFP(-) occur from indels on the three copies of the reporter. Indels are defined broadly in this context as any edits that inactivates the reporter. (c) Representative FACS plots from the EBFP to EGFP conversion experiment. As described in **Fig. 6**, K562 cells stably expressing the EBFP reporter from the *ATP1A1* locus were transfected with PE3max vectors targeting *ATP1A1* exon 4 (pegRNA-Q118R\_v1) and EBFP (epegRNA). Cells were treated (ouabain) or not (untreated) with 100  $\mu$ M ouabain starting 3 days post-transfection until all non-resistant cells were eliminated.  $n = 3$  independent biological replicates performed at different times with equivalent results (See **Fig. 6**).

**a**



**Supplementary figure 24 (Related to Fig. 6). Assessing the impact of complementary-strand nick locations on prime editing byproducts. (a)** PCR-based genotyping of EGFP(+) single cell-derived K562 clones targeted with a PAM-in or a PAM-out configuration. As described in **Fig. 6**, K562 cells stably expressing the EBFP reporter from the *ATP1A1* locus were transfected with PE3max vectors targeting *ATP1A1* exon 4 (pegRNA-Q118R\_v1) and EBFP (epegRNA). Single cell-derived clones were isolated in methylcellulose-based semi-solid RPMI media supplemented with 100  $\mu$ M ouabain and genomic DNA from clones that were EGFP(+) was harvested after coselection. Larger insertions and deletions are indicated.  $n = 17$  single cell-derived clones for each condition from one experiment.

**a****Gating strategy for the mScarlet-I-TOSI assay****Gating strategy for the EBFP to EGFP assay**

**Supplementary figure 25. Gating strategies used during this study. (a)** All cytometry experiments from this study were gated on single cells.

**a**

Figure 5b - uncropped gels

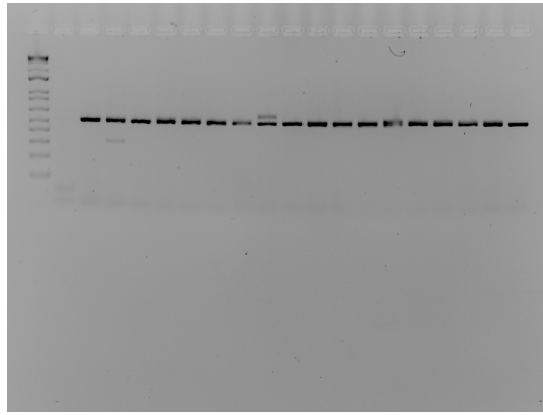
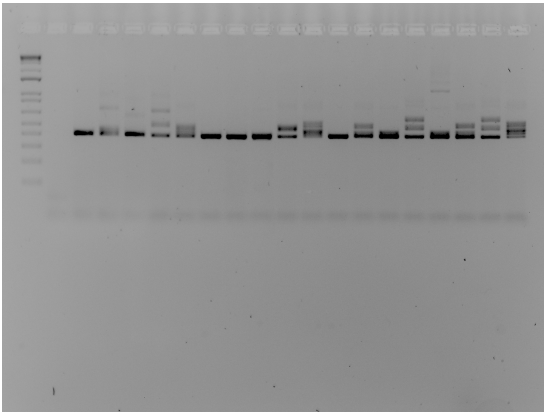


Figure 5c - uncropped gels

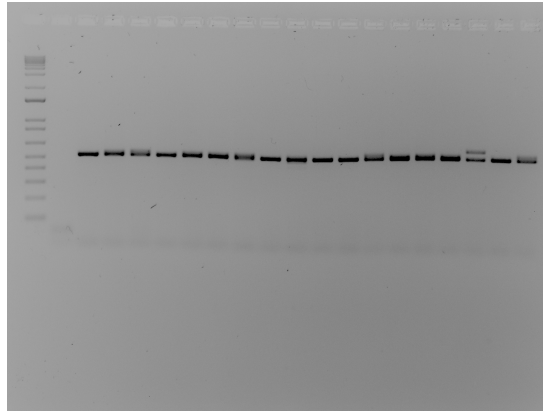
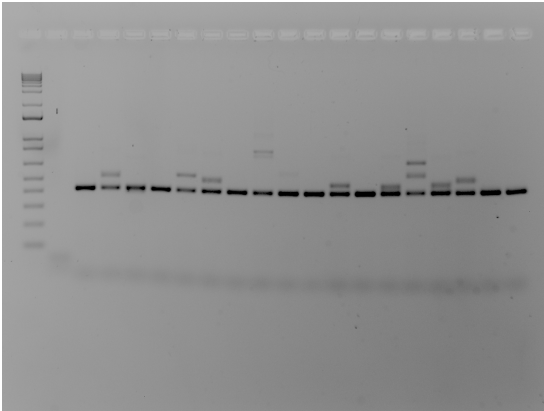


Figure 5e - uncropped gels

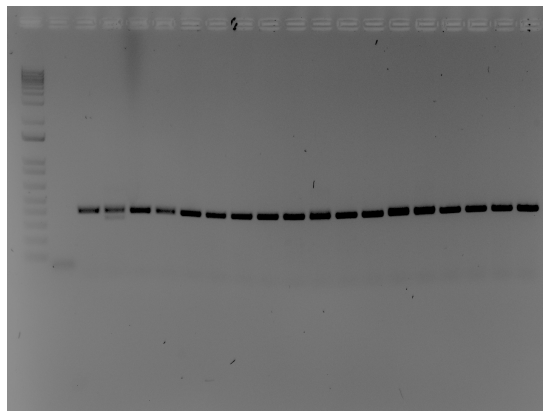
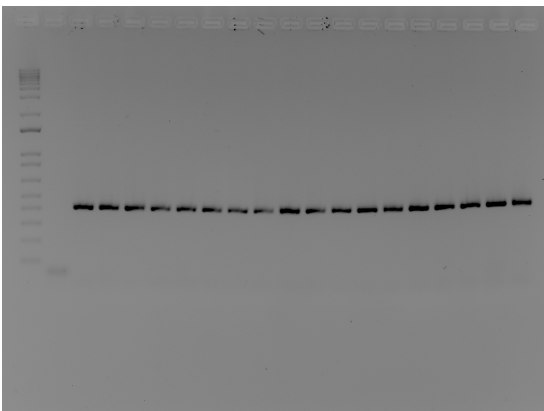
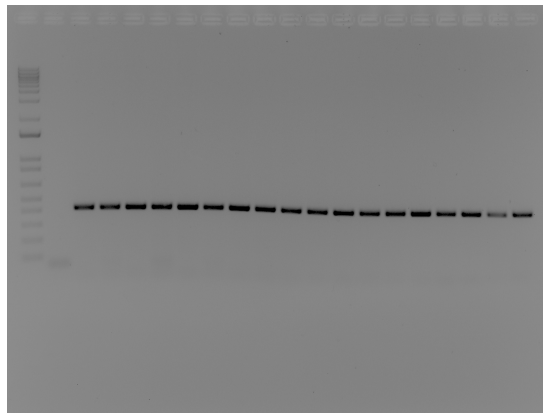
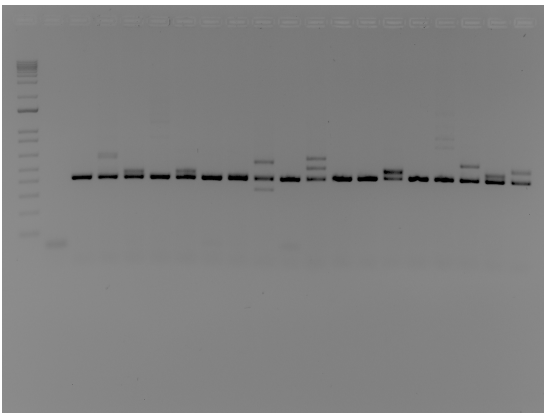




Figure 6d - uncropped gels

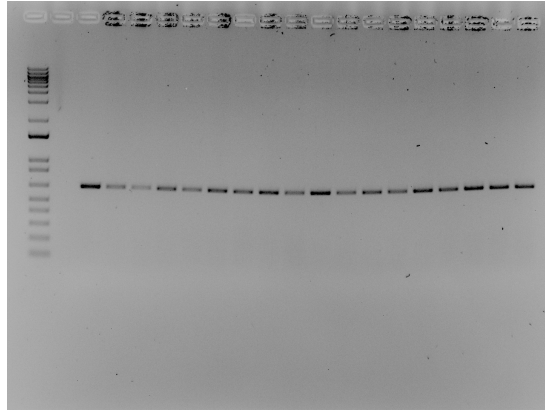
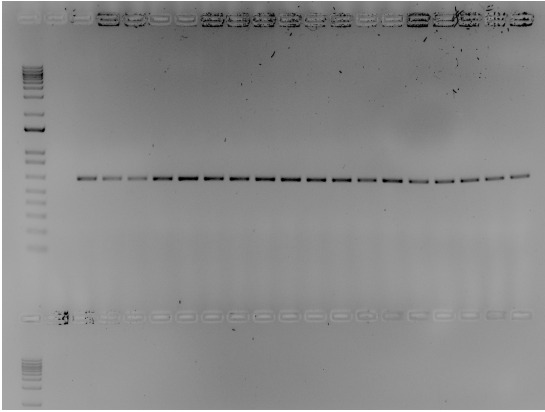
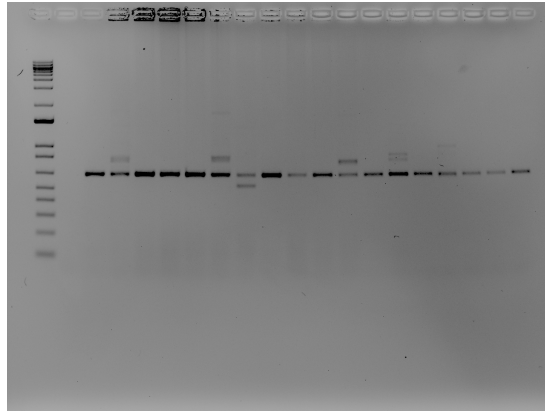
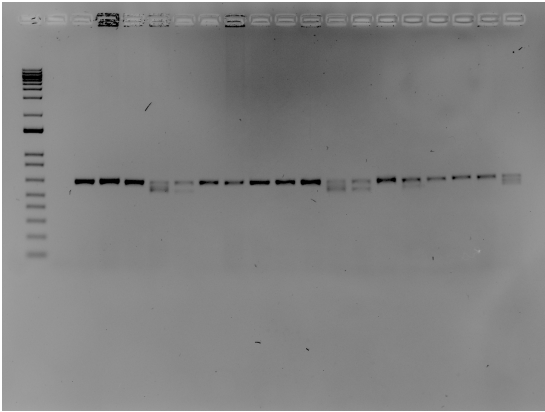
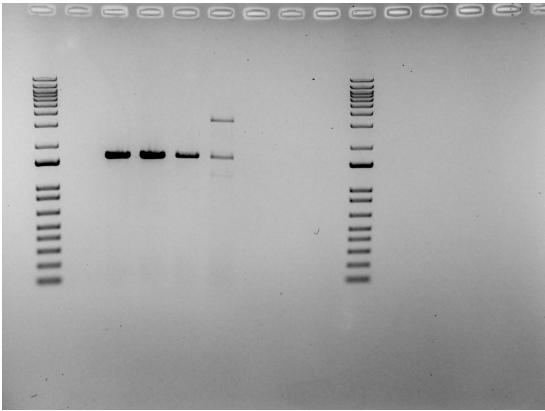


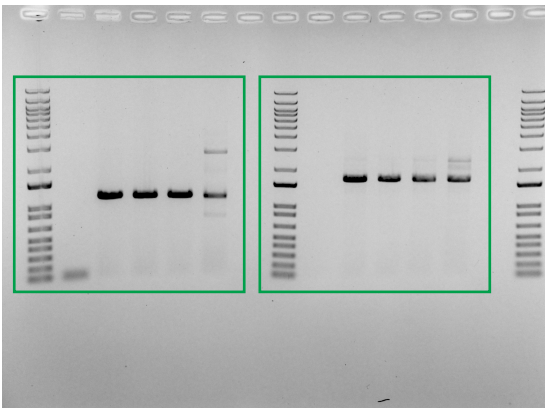
Figure 6e - uncropped gels



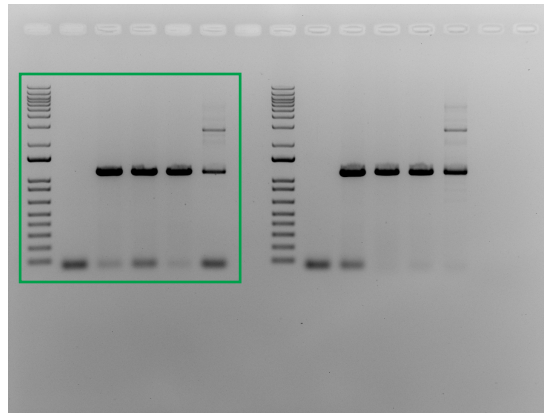
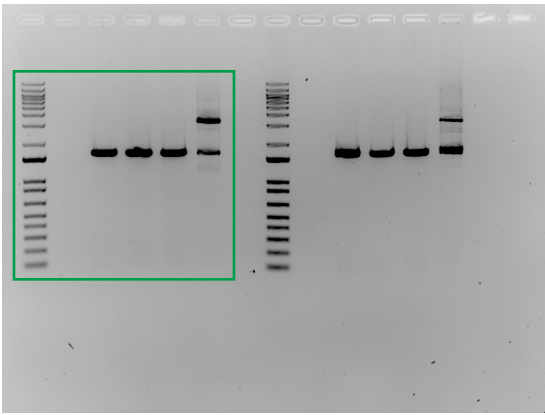
Supplementary figure 2d - uncropped gel



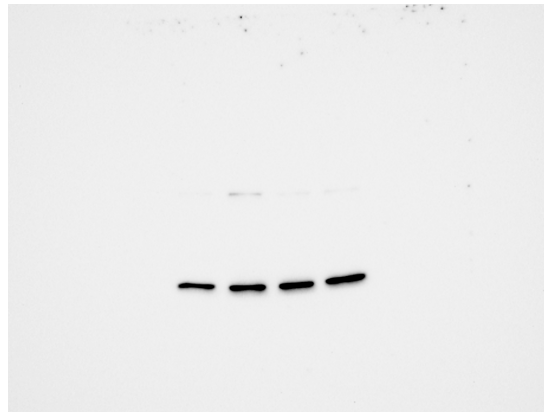
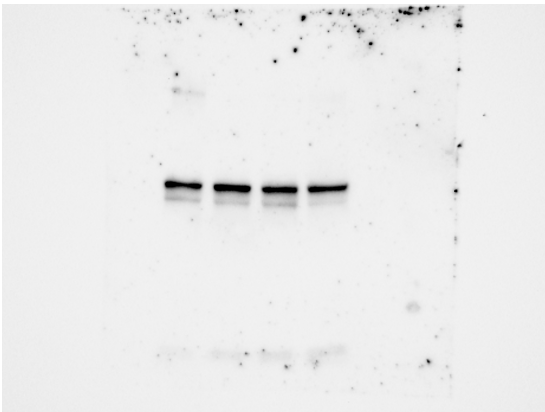
Supplementary figure 3c and 3f - uncropped gels



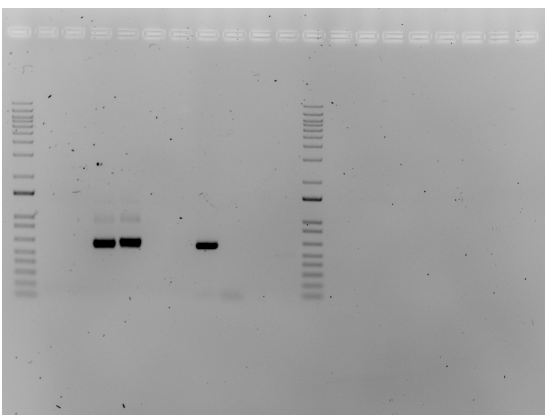
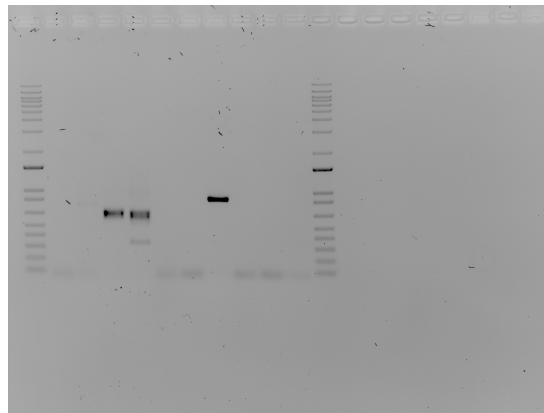
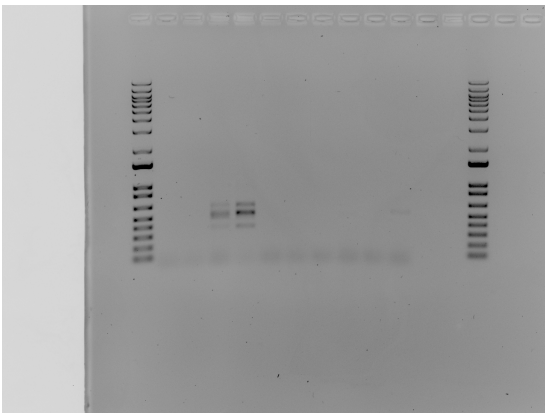
Supplementary figure 4e and 4g - uncropped gels



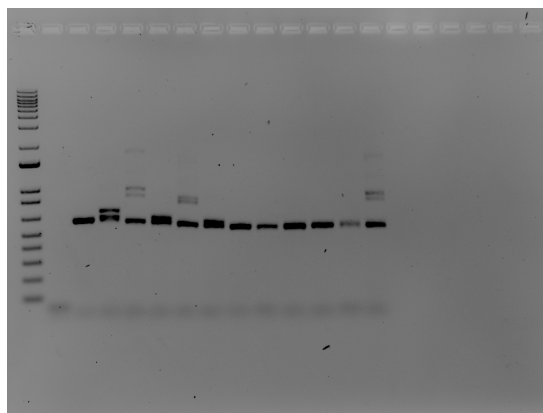
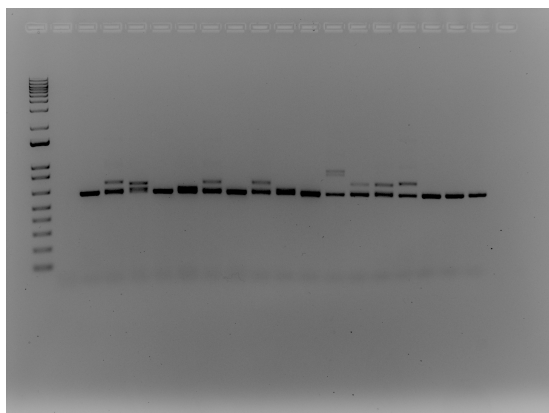
Supplementary figure 7e - uncropped blots



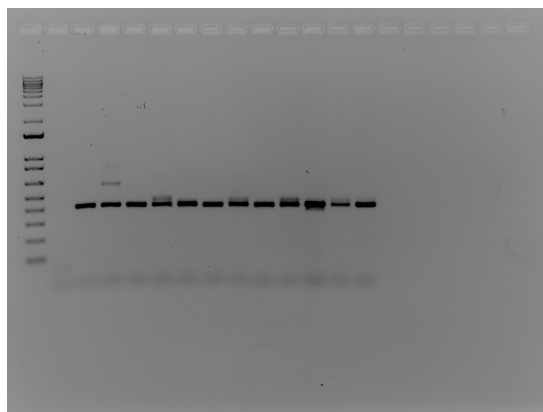
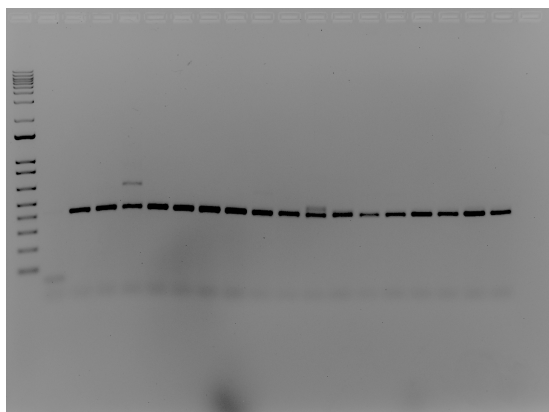
Supplementary figure 9b-d - uncropped gels



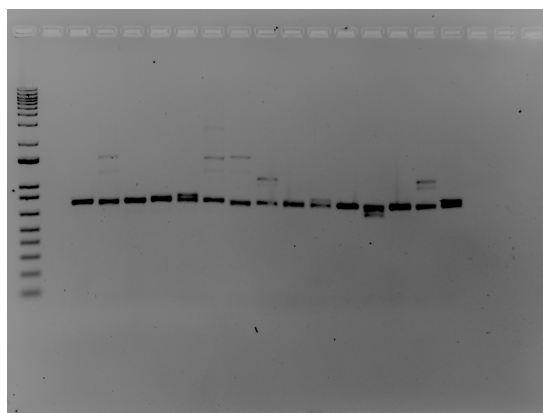
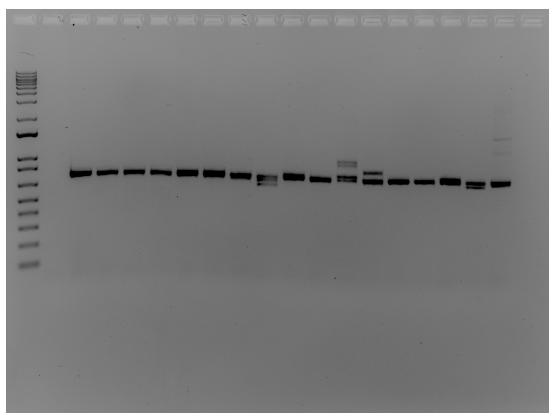
Supplementary figure 14a - uncropped gels



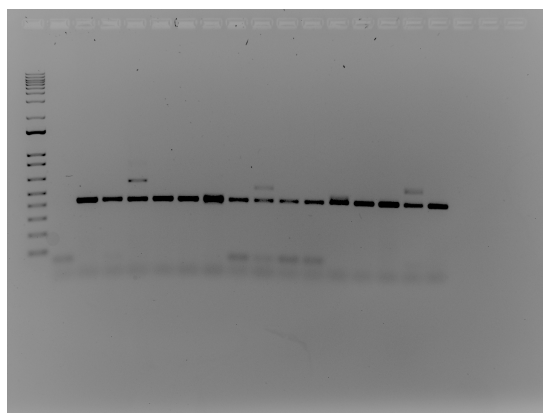
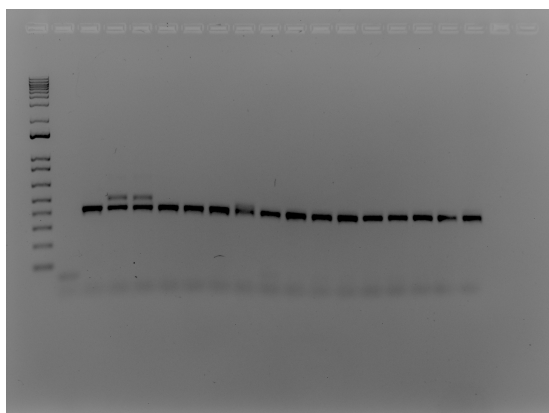
Supplementary figure 14b - uncropped gels



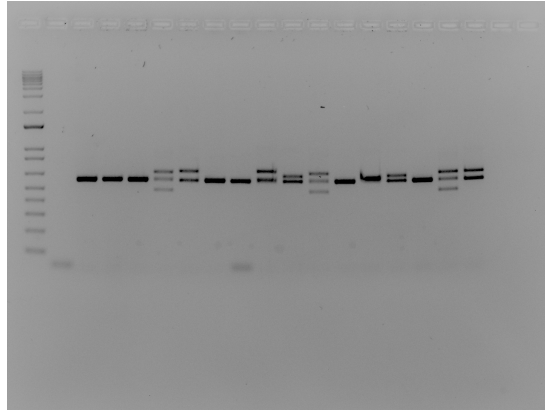
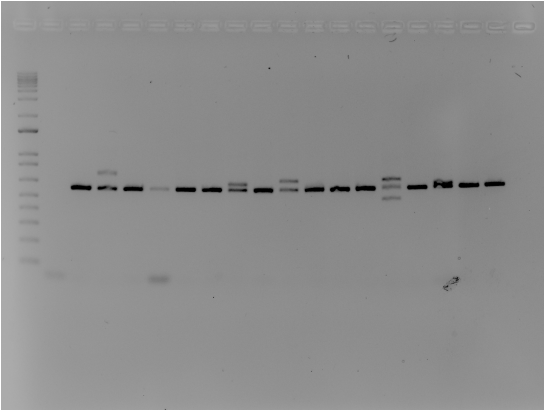
Supplementary figure 14c - uncropped gels



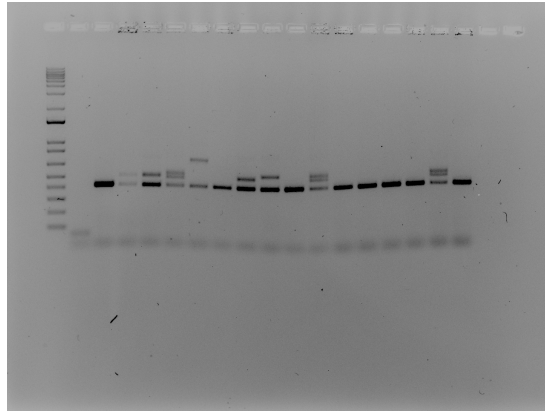
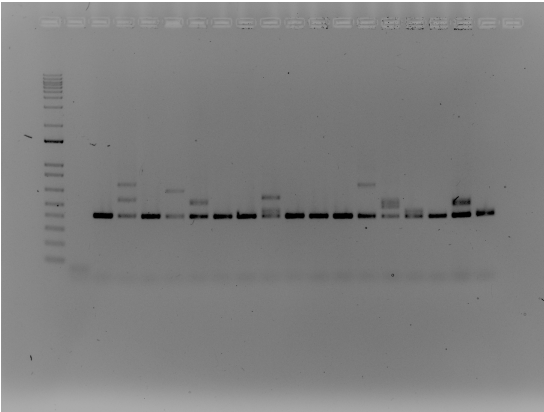
Supplementary figure 14d - uncropped gels



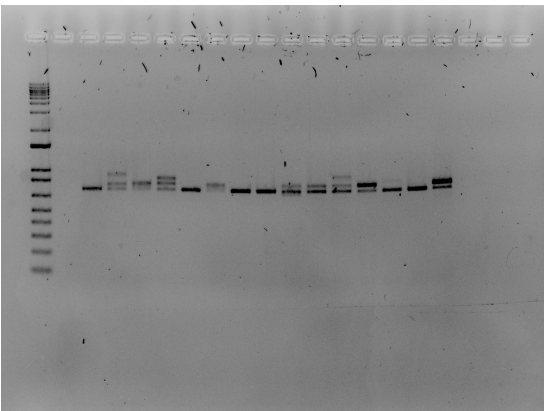
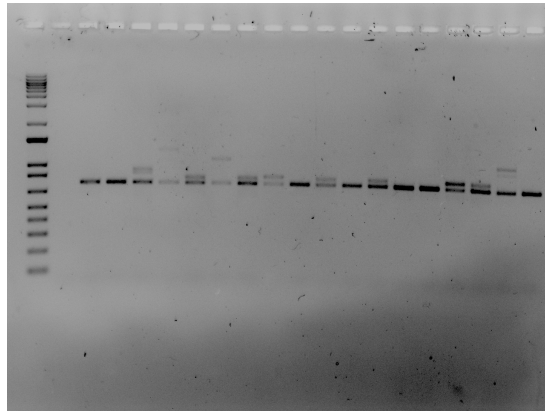
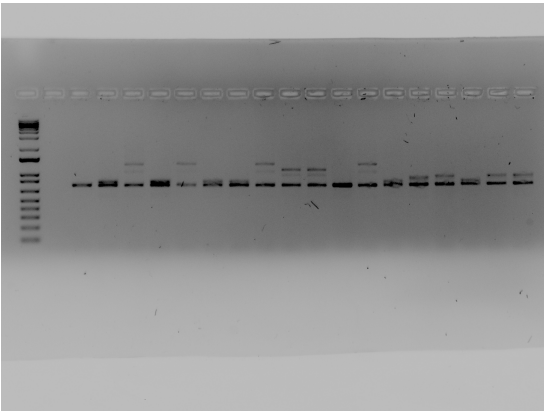
Supplementary figure 14e - uncropped gels



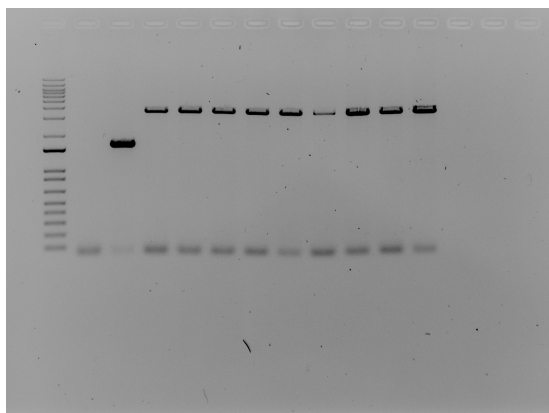
Supplementary figure 14f - uncropped gels



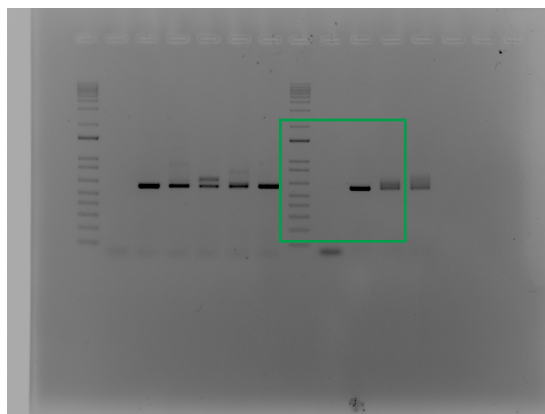
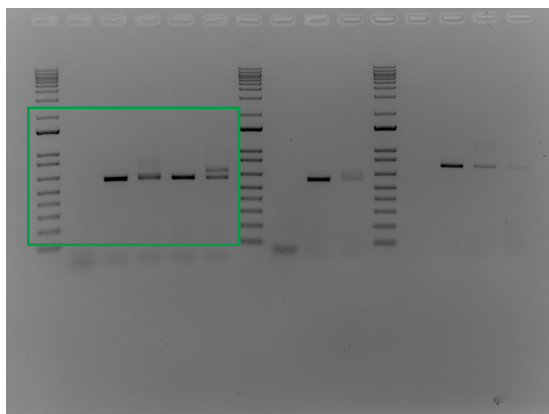
Supplementary figure 14g - uncropped gels



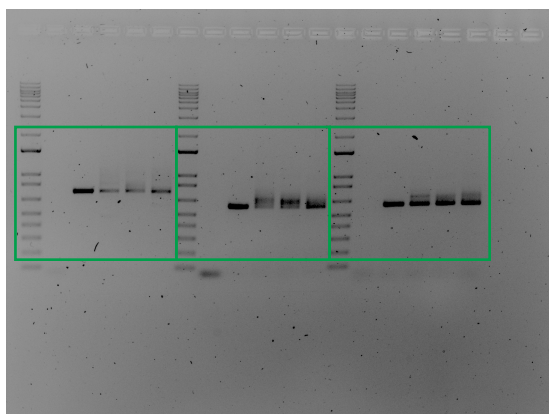
Supplementary figure 15c - uncropped gel



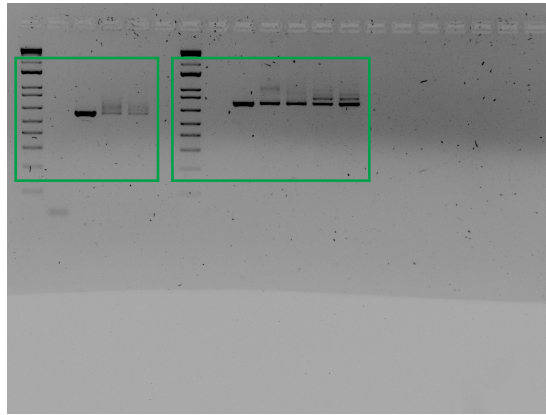
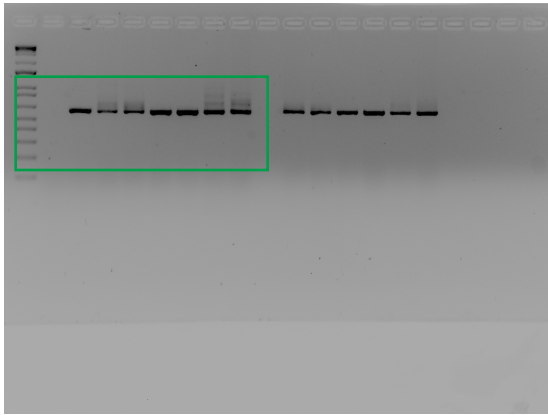
Supplementary figure 17e-g - uncropped gels



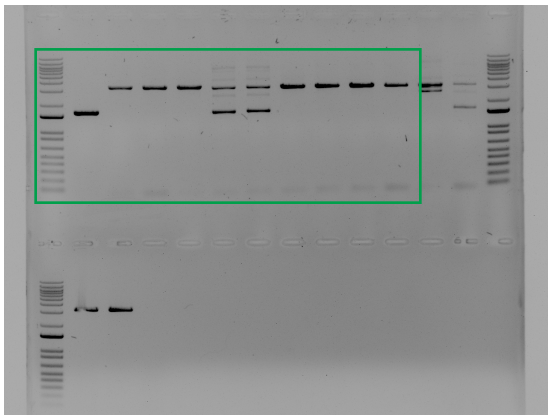
Supplementary figure 21b- uncropped gels



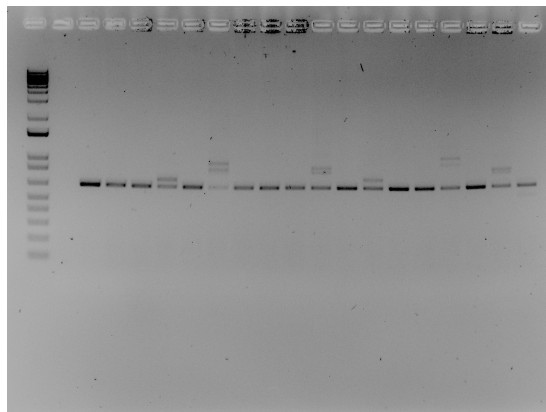
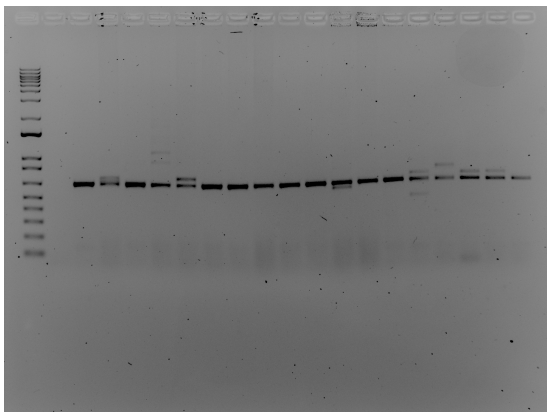
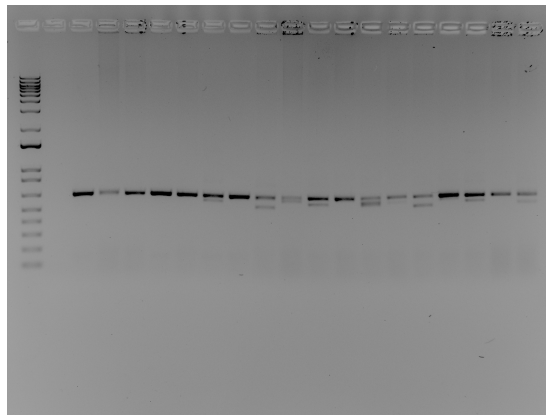
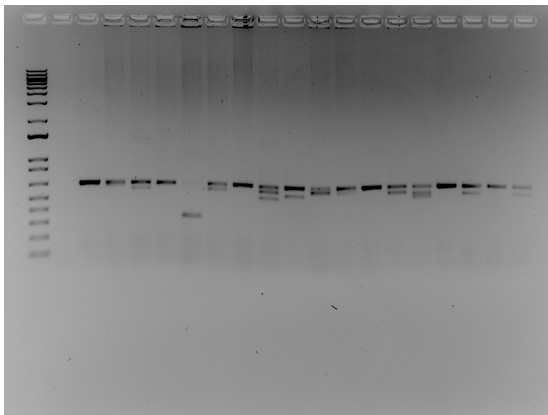
Supplementary figure 21d - uncropped gels



Supplementary figure 22b - uncropped gel



Supplementary figure 24a - uncropped gels



**Supplementary figure 26. Uncropped scans of all gels and blots from this study. (a)** Cropping boundaries from gels harboring more than one experiment are highlighted in green.

**Supplementary table 1: Distribution of alleles in single cell-derived clones edited at *ATP1A1* via prime editing.** K562 cells were transfected with PE vectors targeting *ATP1A1* exon 4 (Q118R). Single cell-derived K562 clones were isolated in methylcellulose-based semi-solid RPMI media supplemented with 0.5  $\mu$ M ouabain and genomic DNA was harvested after coselection. The number of precise prime edited alleles was determined from BEAT Sanger sequencing trace analysis and small insertions and deletions were analyzed with DECODR. PCR-based genotyping was performed to identify larger insertions and deletions.

PE strategy	% of clones with indicated alleles			
	WT + Indels	Monoallelic	Biallelic	Triallelic <sup>&amp;</sup>
PE2-Q118R <sup>*</sup>	0% (0/47)	98% (46/47)	2% (1/47)	0% (0/47)
PE3-Q118R <sup>**</sup>	0% (0/47)	45% (21/47)	40% (19/47)	15% (7/47)

<sup>&</sup>Homozygous, only PE-specified sequences are detected

<sup>\*</sup>No small indels or large insertions and deletions are detected, remaining alleles are WT

<sup>\*\*</sup>For monoallelic and biallelic clones, remaining alleles are WT, small indels or large insertions and deletions. Scaffold incorporations are also detected on PE alleles



**Supplementary table 2: Distribution of alleles in single cell-derived clones edited at *ATP1A1* and *MTOR* by coselection using engineered pegRNAs (epegRNAs) in a PE2 mode.** K562 cells stably expressing the mScarlet-I mTOR Signaling Indicator (mSc-TOSI) reporter were transfected with PE2max-epegRNA vectors targeting *ATP1A1* exon 4 (Q118R) and *MTOR*. Single cell-derived K562 clones were isolated in methylcellulose-based semi-solid RPMI media supplemented with 100  $\mu$ M ouabain and genomic DNA was harvested after coselection. The number of precise prime edited alleles was determined from BEAT Sanger sequencing trace analysis and small insertions and deletions were analyzed with DECODR. PCR-based genotyping was performed to identify larger insertions and deletions.

Targeted locus and mutation	% of clones with indicated alleles			
	WT	Monoallelic*	Biallelic*	Triallelic&
<i>ATP1A1</i> -Q118R	0% (0/20)	10% (2/20)	45% (9/20)	45% (9/20)
<i>MTOR</i> -F2108L	15% (3/20)	20% (4/20)	50% (10/20)	15% (3/20)

\*No small indels or large insertions and deletions are detected, remaining alleles are WT

&Homozygous, only PE-specified sequences are detected